Horizon 2020 Programme
Research and Innovation Action

*This project has received funding from the European Union's Horizon 2020 Research and Innovation Programme, under Grant Agreement **No 773649**.*

Efficient Carbon, Nitrogen and Phosphorus cycling in the European Agri-food System and related up- and down-stream processes to mitigate emissions

Start date of project: 2018-09-01

Duration: 54 months

D3.4. Design and performance of vacuum degasification for agricultural residues and food-waste treatment for nitrogen depletion /recovery

Deliverable details	
Deliverable number	3.4.
Revision number	E
Author(s)	Fabian Kraus, Johannes Koslowski, Jan Schütz, Anne Kleyböcker, Andreas Dünnebeil, Joachim Clemens
Due date	28.02.2023
Delivered date	28.02.2023
Reviewed by	Wim Moerman
Dissemination level	Public
Contact person EC	Violeta Kuzmickaite

Contributing partners	
1.	KWB
2.	PON
3.	SOE

TABLE OF CONTENTS

ACKNOWLEDGEMENT
This work had not been possible without the support of several student assistants, which were qualified via Bachelor or Master Thesis. The Authors express their thank to Lena Geist, Laila Peter, Bastian Schwatke, Tony Rösner, Melina Meng and Felix Gerhardt for their support in the different project stages.

EXECUTIVE SUMMARY
This report summarises the theoretical design of a degasification plant to recover ammonia and carbon dioxide from organic residues, such as agricultural digestates, manure and municipal/industrial wastewater. Heat and water management had been identified as one crucial factor to optimise during this research. The chemical and physical parameters reveal the high tendency of ammonia towards water phase and underline the difficulty in ammonia stripping. Besides temperature, the volumetric gas-liquid ratio had been identified as most important factors. Regarding pH-value it had been observed, that a further increase is not sufficient once pH 9 is reached. Applied absolute pressure also has been identified of lower importance, compared to temperature and volumetric gas-liquid ratio. The latter three parameters are influencing evaporation and heat management in the desorption stage. A design model from literature according to Onda showed good correlation with the practical experiments including packings. Other column fillings as cones lead to operational problems. The understanding of the exact relations in column design are further used to design a cost-efficient process with low carbon footprint. The practical tests, as such, were reproducible, however the batch operation and limitations in the column design resulted in a limited transferability towards large scale plants. In terms of the absorption stage, the pilot needs to be further optimised to reach sufficient recovery rates. An absorption of ammonia and carbon dioxide under use of gypsum is favoured to also recover carbon dioxide and to avoid sulfuric acid dosing. In that term further tests and optimisation is needed, to have a fully quantifiable pilot system. The integration of a measure-control system is a further development step. In conclusion, the degasification process with low pressure (vacuum) reveals benefits compared to conventional air stripping in terms of heat management and the necessary gas-liquid-ratio, which has effects on column diameter and eventually column height. The necessity of aggressive chemicals dosage (as caustic in desorption) or acid (in absorption) is in view of the authors not given, hence cheap and safe alternatives (e.g. CO_2 stripping) and gypsum dosage as alternative sulphur source work sufficient.

1. INTRODUCTION

Residues as agricultural digestates, food waste, food industry wastewater or reject water from municipal sludge treatment are high in ammonium. In terms of agricultural digestate, this ammonium is applied on land. However, in regions suffer from nutrient surplus it is challenging to meet with digestate the specific plant demand at the correct vegetation period. In fact, nutrient demand and supply does not overlap in terms of locality and time [1]. Nutrient excess is leading to emissions such as ammonia (NH_3) and laughing gas (N_2O) and nitrate (NO_3^-) leaching into the groundwater. Within food industry wastewater treatment or municipal sludge treatment, high ammonium loads might be an inhibiter in anaerobic digestion and are removed in anoxic aerobic treatment via a combination of nitrification and denitrification processes [2]. Not only a lot of oxygen and thereby energy is consumed in nitrification, also the formation of laughing gas especially during denitrification is a crucial contributor to climate change. The same applies to denitrification processes in agricultural soil – high loads of unnecessary nitrogen will contribute to climate change by the formation of laughing gas [3]. The European Union tackled this environmental hazard with the nitrates directive and subsequently limited the amount of nitrogen that can be applied to agricultural surfaces to 170 kg of N per ha. To comply with the directive, action must be taken in certain regions mainly in regions with a high share of animal industry, such as the Netherlands or Niedersachsen, GER. Nitrogen management must be applied to farm fertilizers.

The concentration of ammonium is high, so it can be extracted/recovered in form of ammonia via a combined absorption-desorption process from these streams. Conventional Air stripping with pressure can hereby considered as state-of-the-art technology. It requires a desorption and adsorption column, whereby air is loaded with ammonia in the desorption column and unloaded in the absorption column. The cost factors are heat and caustic soda, to move the ammonium-ammonia equilibrium towards ammonia in the desorption column and sulfuric acid for neutralization and harvesting of ammonia in the absorption column. Furthermore, the columns require a feed substrate low in particles, hence the packings within the column tempt to clog in terms of high particle loads. Another technology capable of recovering ammonium is membrane filtration, a pressure driven process where ions are separated through porous interfaces. This technology is very sensitive to high TSS loads and thus cannot be applied to agricultural digestates without excessive pretreatment and operational cost. To achieve ammonium separation from communal waste water, Böhler et al. installed sand filtration, flocculation, lamella clarifier and cartridge filters as necessary steps to achieve a sufficiently clarified substrate for N recovery via membranes [4]. Adsorption to zeoliths via ion exchange (IEX) also is a possibility to remove N from digestate, but lacks large scale application due to an excessive amount of adsorbent needed and substantial fouling problems due to the nature of digestate. [5]

Within this study vacuum degasification or low-pressure stripping was investigated in contrast to conventional air stripping [6]. The claims for this technology were, that it is robust similar to air stripping and therefore realized without the excessive pre-treatment needed for the application of the other addressed technologies. Further the effects of the vacuum on ammonia degasification and its effect on other parameters should be investigated within this study. In detail the following research questions had been investigated:

- How does vacuum degasification effects the water and heat balance of the system? What about steam?
- How do buffer equilibria of digestate effect acid/soda consumption to adjust the pH value?
- How do pH and temperature impact the equilibrium between ions as NH_4^+ and HCO_3^- and gases as NH_3 and CO_2 in solution and in the gaseous phase?
- What process conditions are favorable for desorption and absorption?
- What dimension and height are necessary for a certain recovery target?
- How does different installations (free-fall column, perforated plates and packed column with packings) effect the recovery?
- How were the tests in the pilot unit realized?
- Did theory and experimental results match?
- What are the recommendations for upscaling?
- What are the specific challenges of this technology and how it is assessed in competition to competing technologies?

In the following chapter 2 the theoretical background in terms of water, heat, acid/base equilibrium, gas volatilization, and design guidelines is summarized. Within chapter 3 the experimental results are illustrated and discussed. Chapter 4 summarizes with recommendations for upscaling while in chapter 5 the conclusions are drawn from this report and the technology is compared to competing technologies as air stripping.

2. THEORETICAL BACKGROUND

2.1. Water and Heat balance

As observed in the commissioning phase, water evaporation is a crucial parameter in vacuum degasification operation. The operation with negative pressure and an air stream as transport media results in water evaporation below 100 °C. This has several effects:

1. A high steam content in the gas stream results likely in water absorption in the absorption stage, diluting the product, resulting in lower revenues.
2. Steam generation as such consumes a high amount of thermal energy, that needs to provide via sensible heat, resulting in high operational costs.
3. Steam generation results consequently in a massive temperature decrease at the bottom of the desorption column.

These observations where considered in the following equations and calculations. The third observation may be considered as a positive side-effect of this technology, hence remaining heat can be recovered by accident from the hot substrate. However, without utilization of this generated steam, negative effects occur in the absorption stage and costs for heating increase. Therefore, a design was chosen to re-utilize the heat in steam to increase the temperature of the cold substrate and recycle the heat from the desorption column outflow back to the desorption column inflow. The following equations are illustrating the thermodynamic correlations to identify operational parameter combination to recycle the heat as efficient as possible.

The derivation of the correlation between temperature, absolute pressure and gas-liquid-ratio is outlined in the Annex 7.1. in eq. 10 to eq. 18. The results according eq. 18 are plotted in dependence of temperature and absolute pressure, assuming the substrates initial temperature is around 15° C. The results are shown in Figure 1.

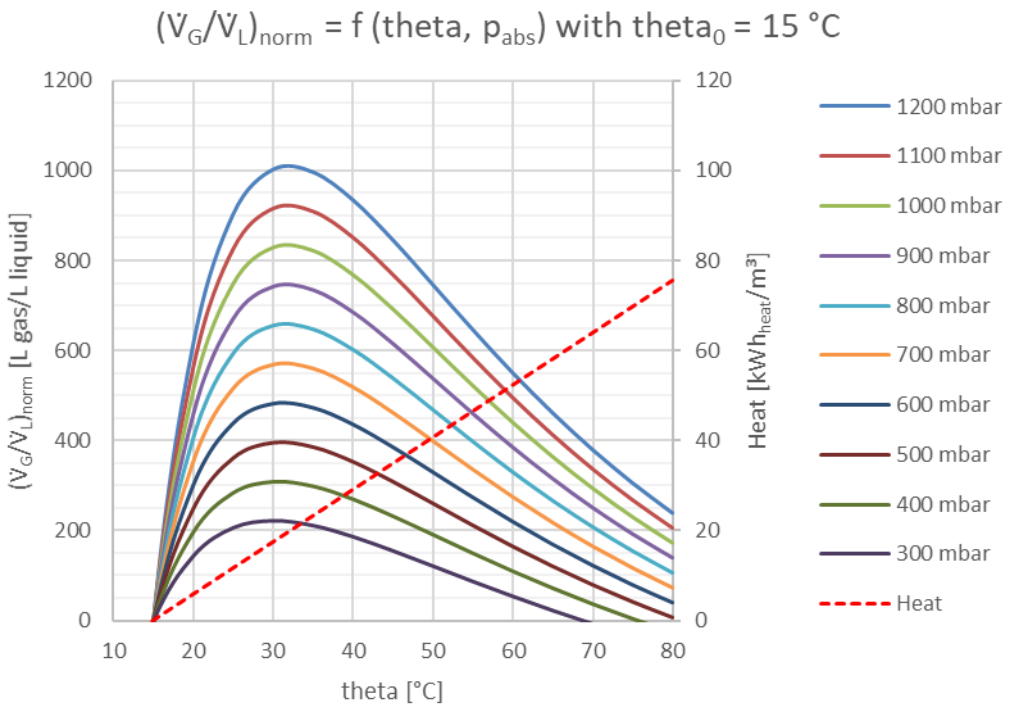

Figure 1: Resulting volumetric gas-liquid-ratio under norm conditions for specific temperature and absoulte pressure conditions within the stripping column maintaining an energetic equilibrium between water evaporation and temperature regime including amount of energy depending on temperature

Figure 1 illustrates resulting gas-liquid-ratios under norm conditions with an initial temperature of the substrate of 15 °C for different temperatures and absolute pressure for an energetic equilibrium between water evaporation and temperature regime. E.g. for a Temperature of 70 °C in the stripping column and an absolute pressure of 900 mbar, a resulting

$(V_G/V_L)_{norm}$ of 250 L/L is calculated to recover a delta T of 55 K in form of steam or to have a steam quantity in the air with its respective latent energy to increase the substrate temperature from 15 °C to 70 °C. With increasing vacuum (decreasing absolute pressure) the resulting $(V_G/V_L)_{norm}$ decreases, hence a too high quantity of steam will be generated. Also the above a temperature of 25 to 35 °C the resulting $(V_G/V_L)_{norm}$ decreases, hence a too high quantity of steam will be generated. The quantity of heat energy of the system is also displayed in Figure 1 revealing a higher energy density of the system with higher temperature and consequently higher steam generation.

2.2. Buffer equilibria and henry's law constant

The buffer equilibria are decisive for the consumption of chemicals to adjust the pH but also interfere with the thermal conditions in the system due to the strong temperature dependence of the NH_4^+/NH_3-system and the effect of stripping gases as CO_2 and NH_3. The Acetate-Buffer of digestate is comparably low due to the degree of degradation in digestion, however it might be relevant if the digestate is acidified. Within this study it is not within the scope. In fact, there are three relevant buffer-systems in the digestate regarding carbonate- and ammonium-species, whereby the carbonate-related systems interfere with each other. The equations are shown in eq. 1 to eq. 3.

$$CO_{2(aq)} + H_2O \leftrightarrow HCO_3^- + H^+ \quad \text{eq. 1}$$

$$HCO_3^- \leftrightarrow CO_3^{2-} + H^+ \quad \text{eq. 2}$$

$$NH_4^+ \leftrightarrow NH_{3(aq)} + H^+ \quad \text{eq. 3}$$

The equilibria are between acid and base are described via pK_A values shown in Table 1. These temperature dependent pK_A-values can be calculated for different temperatures via Van't-Hoffs-Law [7, 8]. Although there is also a dependence from absolute pressure, this is only minor and can be neglected.

Table 1: pK_A values for Carbon Dioxide in Water, Hydrogencarbonate and Ammonium in dependence from temperature [7, 8]

Theta [°C]	10	20	30	40	50	60	70	80
pK_A $[CO_{2(aq)}]$	6,36	6,32	6,28	6,24	6,21	6,17	6,13	6,09
pK_A $[HCO_3^-]$	10,49	10,38	10,29	10,22	10,17	10,14	10,13	10,13
pK_A $[NH_4^+]$	9,74	9,41	9,09	8,76	8,44	8,12	7,79	7,47

As shown in Table 1, there is only a minor distinction for both pK_A-values regarding the carbonate-system between 10 °C and 80 °C. Meanwhile for the ammonium-system, there is a significant decrease of the pK_A-value with increasing temperature from pH 9,74 at 10 °C towards pH 7,47 at 80 °C, which is crucial in terms of desorption.

For the digestate substrate, the following acids and corresponding bases are relevant (see Table 2)

Table 2: Relevant acids and corresponding bases for digestate, their pK_A values and concentrations [9]

Acid/ Base	pK_A	c [mol/L]
H_3O^+/ H_2O	0	55.6
HAc/ Ac^-	4,75	0.05
$CO_{2(aq)}/HCO_3^-$	see Table 1	0.20
$NH_4^+/NH_{3(aq)}$	see Table 1	0.13
HCO_3^-/CO_3^{2-}	see Table 1	0.20
H_2O/OH^-	14	55.6

The buffer capacities according to eq. 19 in the Annex 7.2. are displayed in Figure 2 for a temperature of 15 °C and in Figure 3 for a temperature of 70 °C. At 15 °C two buffer zones can be identified: the first one is around the pK_A of $CO_{2(aq)}$ around pH 6.4, the second around pH 10 evoked by NH_4^+ and HCO_3^-. The pH of digestate is within the "valley" around pH 8. Adjusting the pH of the digestate towards pH 9 requires about 0.07 mol OH/L (respectively 3.2 mL NaOH (50 %)/L) in theory. A further adjustment from pH 9 towards pH 10 requires about 0.16 mol OH/L (respectively additional 8.5 mL NaOH (50 %)/L) in theory. The corresponding experimental determined quantities are 3 mL NaOH (50 %)/L for pH 9 and additional 8 mL NaOH (50 %)/L for pH 10 and fit well to the theoretical numbers. Also after stripping experiments the theoretical and experimental NaOH consumptions towards a pH value of 9 or 10 fit very well.

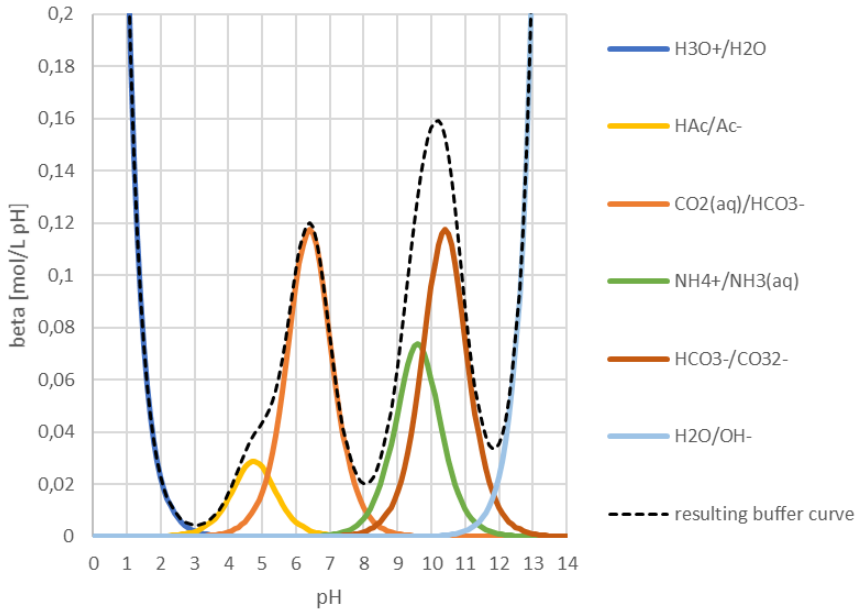

Figure 2: buffer capacity for digestate at a temperature of 15 °C

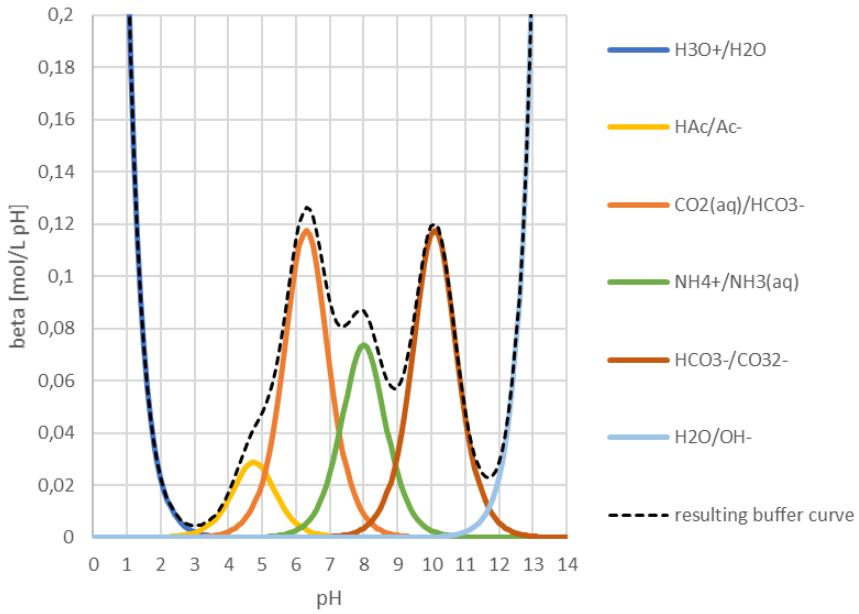

Figure 3: buffer capacity for digestate at a temperature of 70 °C

Due to the temperature dependence of the pK_A of NH_4^+ the buffer correlation changes (e.g. Figure 3), while also the pH of the digestate decreases with increasing temperature. Hence the pK_A of NH_3 is only around pH 8 at 70 °C and a pH-value

up to pH 9 could be easily reached via stripping especially of CO_2 the consumption of NaOH can be easily minimised or even abstained completely.

Considering eq. 20 and eq. 21 in the Annex 7.2. the molar fractions of the acid $CO_{2(aq)}$ and the base $NH_{3(aq)}$ can be calculated in dependency from the temperature dependent pK_A and the pH value. The molar fractions for the gases in solutions are shown in Figure 4.

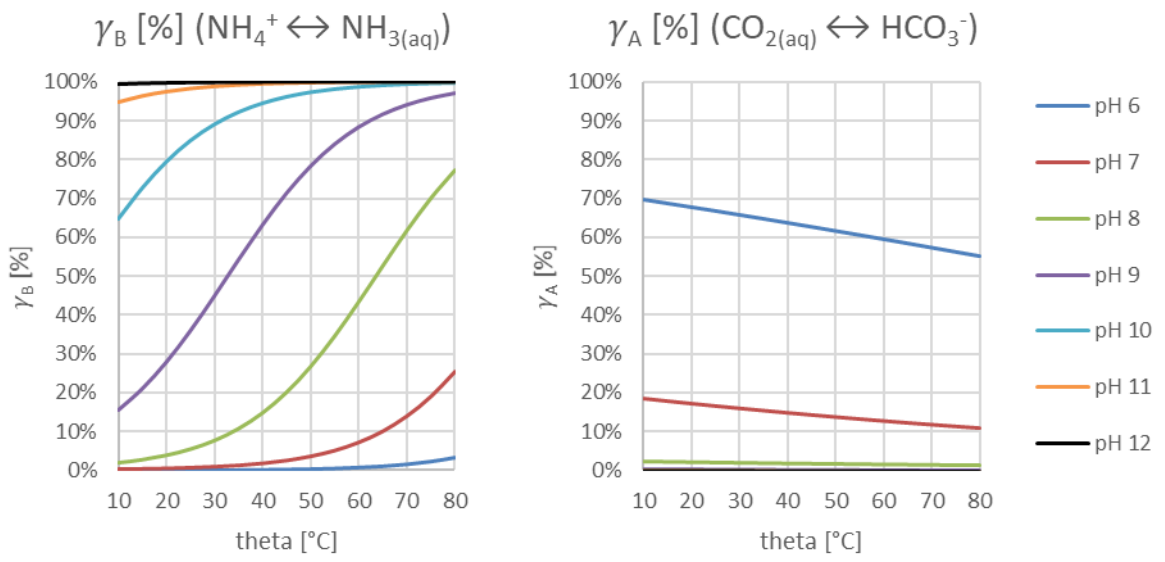

Figure 4: Molar fractions of gases in solution $NH_{3(aq)}$ and $CO_{2(aq)}$ in dependence of temperature and pH-value

Total Ammonia Nitrogen (TAN) is present as NH_4^+ for low pH values around pH 6 and as $NH_{3(aq)}$ for high pH values around 12. In between (especially between pH 7 and 10) the strong temperature dependence of the pK_A value of NH_4^+ strongly effects the equilibrium. E.g. for pH 9 and 70 °C more than 90 % of TAN are present as $NH_{3(aq)}$, whereby for 10 °C only 15 % are present as $NH_{3(aq)}$. In contrast the pK_A value of CO_2 is relatively constant independent from temperature and as a result the molar fraction does not change significantly with the temperature and is only dependent from the pH value.

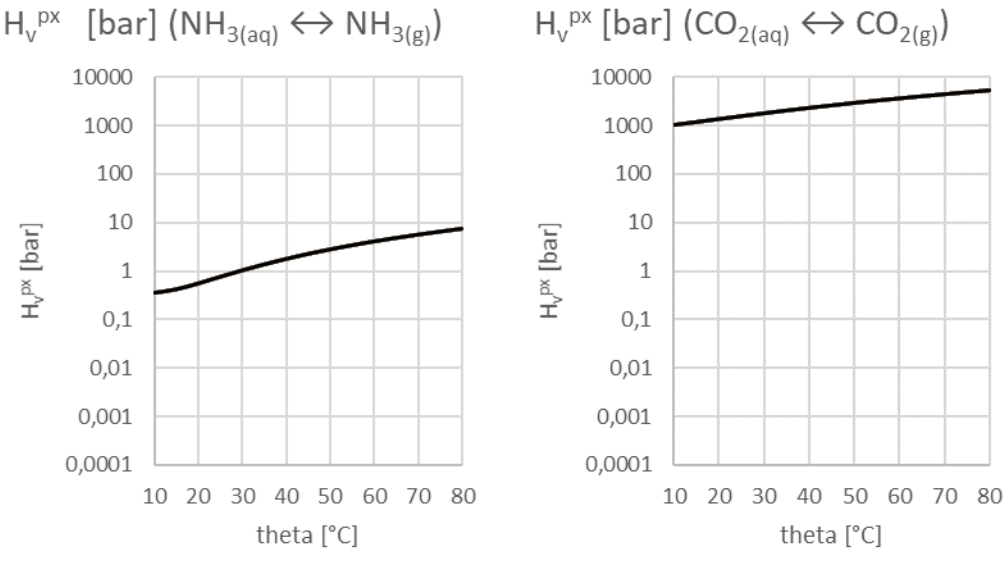

Figure 5: Henry's law constante in bar for equilibria between gases in solution $NH_{3(aq)}$ and $CO_{2(aq)}$ and gases in the gas-phase $NH_{3(g)}$ and $CO_{2(g)}$ [10]

Figure 5 shows the Henry volatility constants (H_v^{px}) for both gases [10]. Ammonia is a highly soluble gas with a water solubility of 514 g NH_3/L for 20 °C or even still 129 g NH_3/L at 70 °C and has accordingly a low H_v^{px} around 0.55 bar for 20

°C and 5.74 for 70 °C. Carbon dioxide is in fact also considered to be a better soluble gas with a water solubility of 1.7 g CO_2/L for 20 °C and 0.37 g CO_2/L at 70 °C compared to other gases as methane, oxygen or nitrogen. The H_v^{px} for Carbon dioxide ranges from 1'384 bar for 20 °C towards 4'548 bar for 70 °C. So roughly the H_v^{px} in bar for Carbon dioxide is by factor 1'000 higher than for Ammonia, which is crucial for the removal of both gases.

Considering both, the presence of gases in solution in Figure 4 and their H_v^{px} in Figure 5, Figure 6 shows the modified Henry's volatility constant for both gases in dependency from their molar fraction ($H_v^{px} \cdot \gamma_{A/B}$). For ammonia, $H_v^{px} \cdot \gamma_B$ is almost independent from the pH value between pH 10 and 12. Even for pH 9 $H_v^{px} \cdot \gamma_B$ aligns towards the maximum for temperatures around 70 °C. In fact temperature is the most important factor, once a pH around pH 9 is reached. In contrast, $H_v^{px} \cdot \gamma_A$ for CO_2 is by far more pH and less temperature dependent. Even at pH 9 the product from Henry volatility constant and molar fraction is higher for carbon dioxide than for ammonia. As a consequence, temperature and pH value should be chosen on behalf on ammonia's equilibrium considering also water and heat balance, material stability and consumption of caustics. Considering the proton consumption during carbon dioxide stripping and proton release during ammonia stripping, both gases are in a equlibrium for 70 °C at a pH value of pH 9.2. This pH was not reached during the batch experiments due to insufficient CO_2 removal as a result of a low volumetric gas-liquid-ratio. Accordingly, the resulting equilibrium pH value for 10 °C (absorption stage) for both gases without additives (acids or gypsum) is pH 10.1.

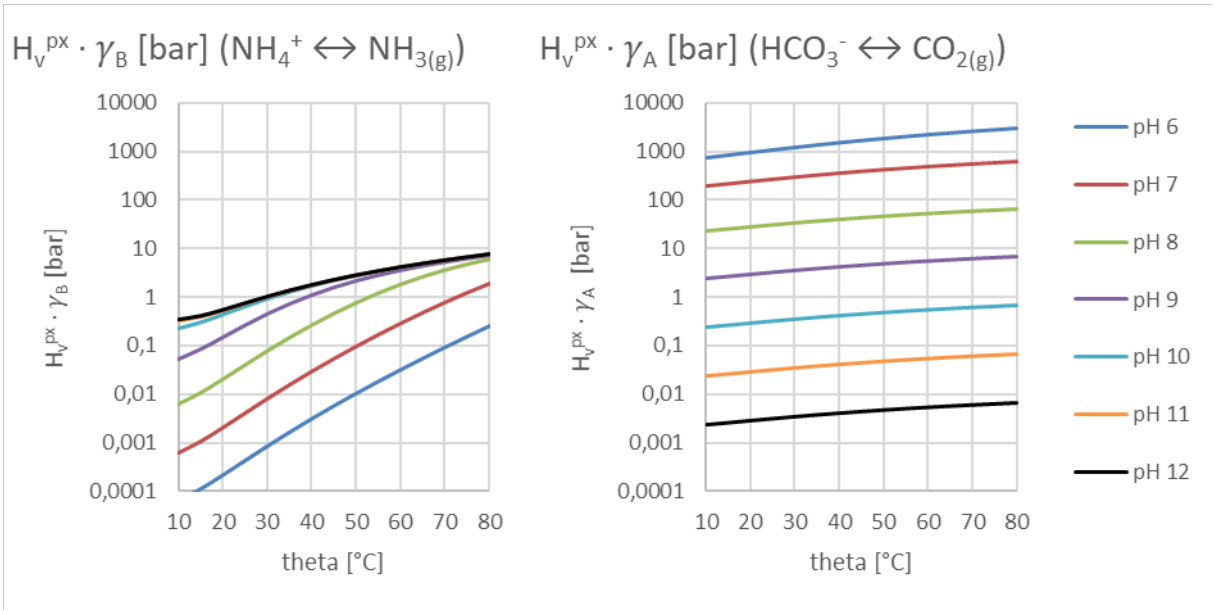

Figure 6: modified Henry volatility constants considering molar fractions in bar for equilibria between ions in solution NH_4^+ and HCO_3^- and gases in the gas-phase $NH_{3(g)}$ and $CO_{2(g)}$

2.3. Calculation of desorption and absorption stage

Remark: *if not explicitly mentioned with an index "d" (for desorption) or an index "a" (for absorption) the following equations are valid for desorption and absorption and must be calculated independently from each other for the specific conditions in the desorption and absorption column.*

The molar fraction of the corresponding NH_3 or CO_2 in the gas (air) y_i is thereby according to Henry's law dependend from the molar fraction NH_4^+ or HCO_3^- in the liquid (substrate or water) x_i, Henry's law constant H_v^{px}, the molar fraction of NH_3 or CO_2 in relation to Total Ammonia Nitrogen or Total Carbonate species $\gamma_{A/B}$ and from the absolute pressure p_{abs} [11].

$$y_i = x_i \cdot \frac{H_v^{px} \cdot \gamma_{A/B}}{p_{abs}} \leftrightarrow x_i = y_i \cdot \frac{p_{abs}}{H_v^{px} \cdot \gamma_{A/B}} \quad \text{eq. 4}$$

y_i	Molar fraction of i in gas	$\mathrm{mol/mol}$
x_i	Molar fraction of i in liquid	$\mathrm{mol/mol}$
$\gamma_{A/B}$	Molar fraction of acid/base in relation to total substance	$\mathrm{mol/mol}$
H_v^{px}	Henry volatility constant for substance i	bar
p_{abs}	Absolute pressure of the system	bar

Following eq. 4 a so called “equilibrium-line” can be calculated for various given x_i and resulting y_i in case of desorption and for various given y_i and resulting x_i in case of absorption. The gradient of the equilibrium line is given in eq. 5 [11]:

$$m_{eq} = \frac{H_v^{px} \cdot \gamma_{A/B}}{p_{abs}} \qquad \text{eq. 5}$$

$m_{eq,d/a}$	Gradient of the equilibrium line for absorption or desorption	$-$
$\gamma_{A/B}$	Molar fraction of acid/base in relation to total substance	$\mathrm{mol/mol}$
H_v^{px}	Henry volatility constant for substance	bar
p_{abs}	Absolute pressure of the system	bar

The operational balance of incoming and outgoing substances can be described as balance beetween influent x_{in} and effluent x_{out} in the liquid L and influent y_{in} and effluent y_{out} in the gas G. For the desorption it is given in eq. 6 and for the absorption it is given in eq. 7. According to these equations a so called “operation line” can be calculated [11].

$$L_d \cdot (x_{in,d} - x_{out,d}) = G \cdot (y_{out,d} - y_{in,d}) \qquad \text{eq. 6}$$

$$\leftrightarrow y_{out,d} = \frac{L_d}{G}(x_{in,d} - x_{out,d}) + y_{in,d}$$

L_d	Liquid load in the desorption stage	$\mathrm{kmol/h}$
G	Gas load	$\mathrm{kmol/h}$
$x_{in,d}$	Influent concentration in the liquid in desorption	$\mathrm{mol/mol}$
$x_{out,d}$	Effluent concentration in the liquid in desorption	$\mathrm{mol/mol}$
$y_{in,d}$	Influent concentration in the gas in desorption	$\mathrm{mol/mol}$
$y_{out,d}$	Effluent concentration in the gas in desorption	$\mathrm{mol/mol}$

$$L_a \cdot (x_{out,a} - x_{in,a}) = G \cdot (y_{in,a} - y_{out,a}) \qquad \text{eq. 7}$$

$$\leftrightarrow x_{out,a} = \frac{G}{L_a}\left(y_{in,a} - y_{out,a}\right) + x_{in,a}$$

L_a	Liquid load in the absorption stage	kmol/h
G	Gas load	kmol/h
$x_{in,a}$	Influent concentration in the liquid in absorption	mol/mol
$x_{out,a}$	Effluent concentration in the liquid in absorption	mol/mol
$y_{in,a}$	Influent concentration in the gas in absorption	mol/mol
$y_{out,a}$	Effluent concentration in the gas in absorption	mol/mol

In a combined desorption-absorption process with circulated gas stream between desorption stage and absorption stage $y_{out,d}$ is equal to $y_{in,a}$ and $y_{out,a}$ is equal $y_{in,d}$.

For given x_{in} and y_{in} corresponding x_{out} for absorption or y_{out} for desorption can be calculated in dependence from given y_{out} for absorption and x_{out} for desorption defined via the targetet recovery rate for desorption and absorption. Based on that operation lines can be calculated as illustrated in Figure 7.

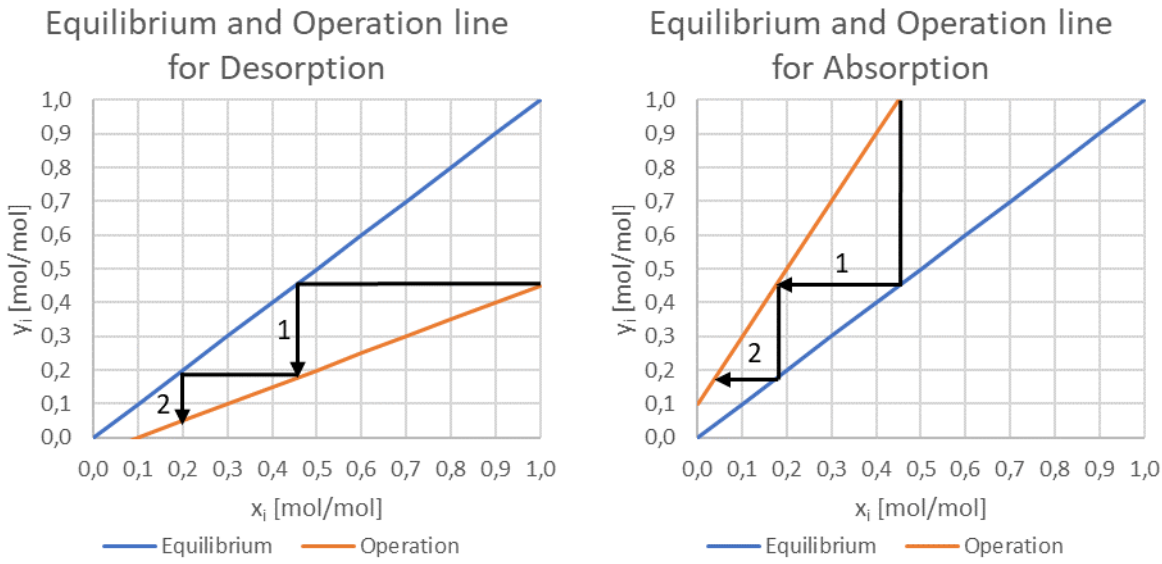

Figure 7: McCabe-Thiele Diagrams with Equilibrium line and Operation line for Desoption and Absorption with two theoretical plates for a hypothetical recovery of about 80 %.

In terms of desorption the operation line should be below equilibrium line, in case of absorption the operation line should be above the equilibrium line. If operation line crosses the equilibrium line, recovery is only possible to a certain x_i or y_i where the lines are crossing. The following calculation of theoretical plates, heigh equivalent of one theoretical plate and heigh of packings are detailed described in the Annex 7.3. in eq. 22 to eq. 37 [11].

2.4. Pressure loss of column

As illustrated in the Annex 7.4. in eq. 38 to eq. 46 the pressure loss is dependent from several parameters, such as the column diameter, the packings and the gas and liquid load of the column. Figure 8 and Figure 9 show examplary the pressure loss for a column with 20 cm diameter for desorption and absorption. However these diagramms are not significant different for other diameters, hence the gas load factor considers the gas velocity and thereby the column

diameter. For negligeble gas load factors and gas streams the pressure loss is constant is for a specific type of packings and temperature. After a certain gas load factor of approximately 0.01 (equivalent to a norm gas volume flow of 1 m³/h, operated at an absolute pressure of 900 mbar and a column diameter of 20 cm), the pressure loss per column height increases with the gas load factor and the gas volume flow. Until a gas load factor of 0.1 (equivalent to a norm gas volume flow of 10 m³/h, operated at an absolute pressure of 900 mbar and a column diameter of 20 cm), the pressure loss is almost independent from the liquid load in the column. Afterwards the liquid load has sever impact on the pressure loss, due to the effect that gas and liquid load are sufficient high, that friction is present. Figure 8 (right) highlights the operational conditions relevant for the desorption column. The gas load factor of the VD is set between 0.2 and 1, resulting in a pressure loss of 0.1 and 2 mbar/m. With decreasing gas-liquid-ratio and increasing liquid load the pressure loss increases, however within this operational boundary, the increase is not that sever.

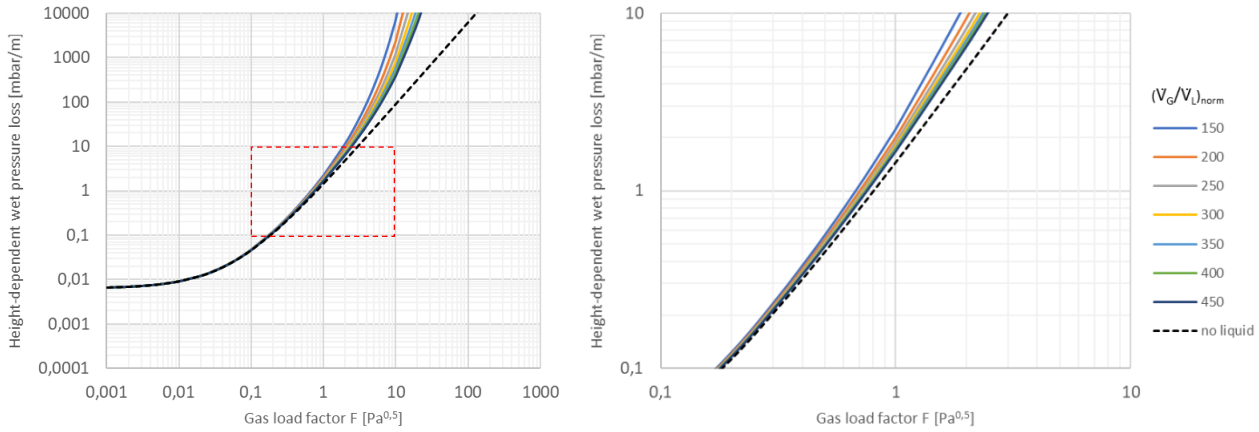

Figure 8: Height-dependent pressure loss in dependency of gas load factor for desorption

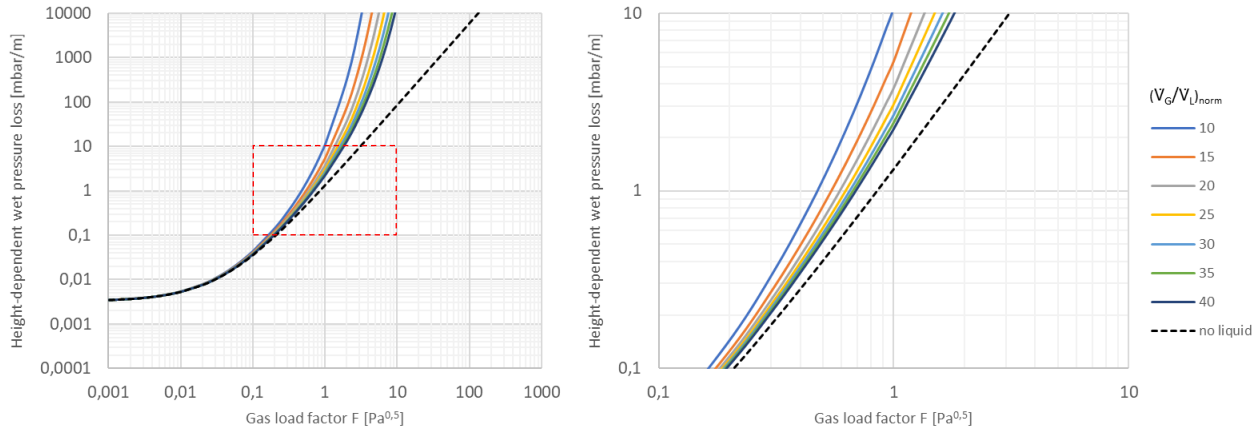

Figure 9: Height-dependent pressure loss in dependency of gas load factor for absorption

In terms of absorption, the temperature and thereby the viscosity of liquid and gas influence the pressure loss. Furthermore the lower gas-liquid-ratio, e.g. the high liquid load of the absorption results in higher pressure losses for a given gas load factor of 0.2-1. The pressure loss for an operation with a preffered gas-liquid-ratio of 20-25 is with around 0.1-4 mbar/m in the range recommended by literature [11].

Different packings have results on pressure loss, via their specific surface area and their porosity. The porosity in terms of an empty column with low gas load factor (and low liquid load) the pressure loss is for large packings with less specific surface area lower and for small packings with higher specific surface area higher. However when the column is highly loaded, the high liquid load significantly effects the pressure loss. The empty spaces between large packings are easilier filled with liquid therefore the pressure loss increases (see Figure 10 for a typical desorption column). In Figure 10 for desorption it became apparent that the pressure loss is lower in the gas load range of 0.1-1 for large packings. However

for absorption with lower gas-liquid-ratio this is different. Here large packings lead to higher pressure losses, due to the high liquid load within the empty spaces between fittings.

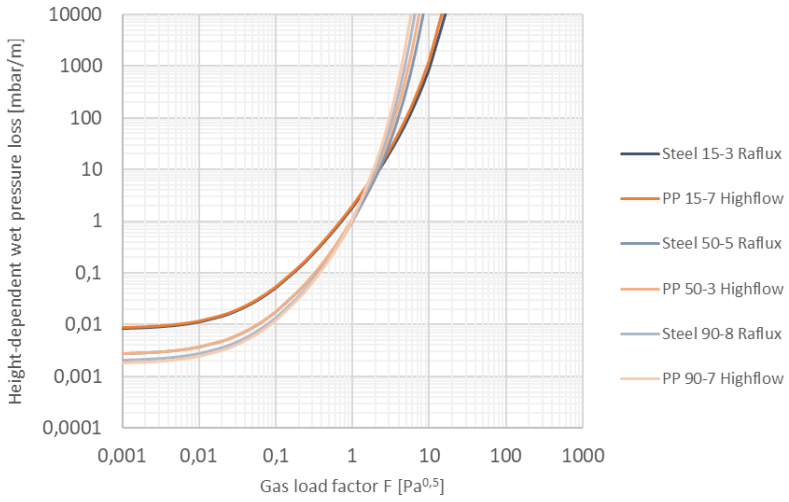

Figure 10: Height dependent pressure loss for a fixed gas-liquid-ratio and different packings

3. EXPERIMENTAL RESULTS

The initial idea for PONDUS-N traces back to the established process of vacuum degassing to remove residual methane in biogas sludge. It is deployed to force out methane traces for a greater efficiency of the overall process, not only leading to optimized valorisation of energy potential but also reducing negative effects of gas bubbles in the post-thickening process [12]. Since ammonia, just as methane, is also a gas residual in digested organic matter, a similar approach to remove it can be applied. Different behaviour in regards to solubility and substance equilibrium have to be considered.

The tests were mainly carried out in four series, based on findings in the previous tests:

A commissioning of the degasification unit using the initial design
B testing of free fall column to reduce hydraulic problems in the reactor (with simultaneous testing of steam recovery through different means)
C testing of a packed bed column to increase the elimination rate
D commissioning of absorption unit using the initial design (with additional testing of an experimental loop reactor as a different approach to recover ammonia)

Design changes are shown in the flow scheme of the respective test series.

Experiments were carried out in threefold repetition if not otherwise indicated. The test parameters were temperature, pH value and absolute pressure as well as the norm volume flow of the air used for stripping purposes.

The batch tests were prepared by packing the column sump that was used as a intermediate batch storage during the tests with digestate (V = 35 L). While packing $NaOH_{50\,\%}$ was added to adjust the pH value, the necessary amount was titrated using the raw liquid digestate before each experiment. After the heater was heated up to the desired temperature, the experiment was initiated by starting the recirculation of the digestate and turning on the vacuum pump. After the system pressure and stripping gas flow reached the designated values, the first sample was taken and the timer of the experiment was started. Samples were taken depending on the experiment setup. Exact times can be taken from the associated dataset and are indicated in the illustrative graphics. In some experiments, the test parameters were changed during the run to see the effect on related things like the simultaneous removal of CO_2 in the digestate.

Parameters investigated in the samples were pH value, TAN, TIC and DR. Additionally operating parameters were tracked manually (temperature at column entry, temperature at sampling point, absolute pressure, volume flow of stripping air, temperature of the absorbtion fluid). Not all parameters were collected in all test series; the relevant data was set iteratively.

TAN and TIC were analyzed using a Hach Lange photometric cuvette test system. The digestate was centrifuged for 10 min at 4000 rpm to reduce coarse particles and diluted to the suitable test range. After that, tests were prepared according to the manufacturer's instructions (Table 3). The DR was tested by an external laboratory associated with the Institute for Agro- and Urban-ecological Projects of the HU Berlin (IASP) using the standard DIN method (drying at 105 °C for 24 h).

Table 3: Used cuvette tests

Name	Parameter
LCK 303	NH_4-N
LCK 388	Carbonate (as CO_2)

The sensors and devices used to collect, analyze and prepare test data are shown in Table 4.

Table 4: Used sensors and laboratory equipment

Name	Application
Hach Lange® DR 3800	Photometer
Hach Lange® HT 200 S	Laboratory heater

Premiere® XC-2450 Series	Laboratory centrifuge
WTW® pH 3210	pH measurement
WTW® LF 340	EC and sample temperature measurement
ifm TN2445	Temperature measurement at sampling point and column head
ifm PG2895	Pressure measurement
Krohne VA40	Air flow measurement

For test series A, digestate from Havellandhof Ribbeck GbR in Ribbeck (Nauen), Germany was used, while for series B to D digestate was obtained from Agro Farm Nauen GmbH (Nauen, Germany). Fluctuations in initial TAN content originate from different batches, aged batches and non-chronological representation.

Regarding the statistical evaluation of the analyzed results, the triplicates were testes with Dixon's Q-test for sample size n = 3 with a confidence of 90 % and Q_{crit} = 0.941. If the hypothesis was confirmed, a single outlier was eliminated and not further used for visualization or evaluation. Errorbars indicate the standard deviation.

3.1. Preliminary laboratory tests

Before the initial commissioning of the pilot unit was carried out starting early/mid 2020, laboratoy batch tests were conducted to gain understanding of the underlying physiochemical mechanics of the degasification process [13]. Suitable parameters were extracted from literature [8], who used comparable conditions in laboratory experiments.

For the trials round-bottomed flasks filled with 2500 mL hand-sieved non-separated digestate was placed in a water bath and heated 60 °C. The pH was adjusted using sodium hydroxide to the desired value (8 to 9.5) and kept at this value by adding NaOH during the experiment, if it dropped. A laboratory vacuum pump was attached. For 4 of the 5 presented experiments the absolute pressure was set to 190 mbar, for the last experiment to 300 mbar. The test duration was 120 min. If not otherwise indicated by errorbars, tests were only carried out once. The results of the preliminary laboratory experiments are depicted in Figure 11.

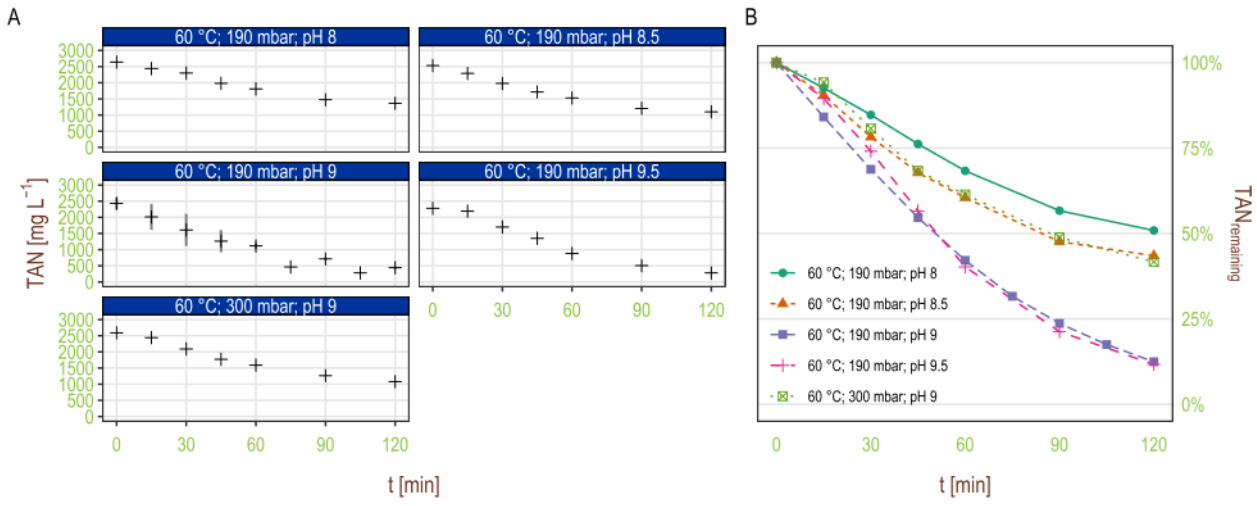

Figure 11: (A) Preliminary laboratory batch tests, at 60 °C multiple tests have been conducted at different absolute pressures and pH levels; (B) comparison of fitted TAN eliminations

It was determined that the degasification of ammonia in batch setups can sufficiently be described as a reaction of 1. order kinetics, this means the initial concentration of ammonia in the substrate does not have any impact on the degasification rate. It becomes apparent, that the pH value at constant temperature and pressure increases the degasification rate. At pH 8, only 49 % of the initial TAN could be removed, while at pH 8.5 and 9 higher eliminations could be achieved (57 % respectively 87 %). A pH of 9.5 did not yield a significantly higher elimination (88 %). At pH 9 using an absolute pressure of 300 mbar in comparison to 190 mbar, the achieved elimination was significantly lower (58 % instead

of 87 %) (Table 5). 60 °C/190 mbar are boiling point conditions for H_2O. To find a universal expression for the degasification efficiency, the half-life is used. Like the 120 min time it clarifies, that a pH above 9 at the given condition does not yield a significantly better performance. Ammonia from the gas stream was recovered in sulphuric acid to form di-ammonia sulphate, but the results are not of greater importance for the rest of the piloting process and thus not included. Overall from the laboratory results it could be derived, that a pH of 9 at the given parameters (60 °C; 190 mbar) was a suitable choice for the objective to remove ammonia with a high efficiency.

Table 5: Test parameters and TAN elimination of selected laboratory tests

Laboratory test	1	2	3	4	5
T [°C]	60	60	60	60	60
p [mbar]	190	190	190	190	300
pH	8.0	8.5	9.0	9.5	9.0
TAN_{elim} (120 min)	49 %	57 %	87 %	88 %	58 %
$t_{50\,\%}$ [min]	124	99	41	39	96

3.2. Construction and design of initial VD-pilot unit for N-recovery

The basic concept of the PONDUS-N pilot unit consists of three stages:

1. Reception, pre-treatment and storage of digestate
2. Vacuum degasification
3. (Neutral-)acidic absorption

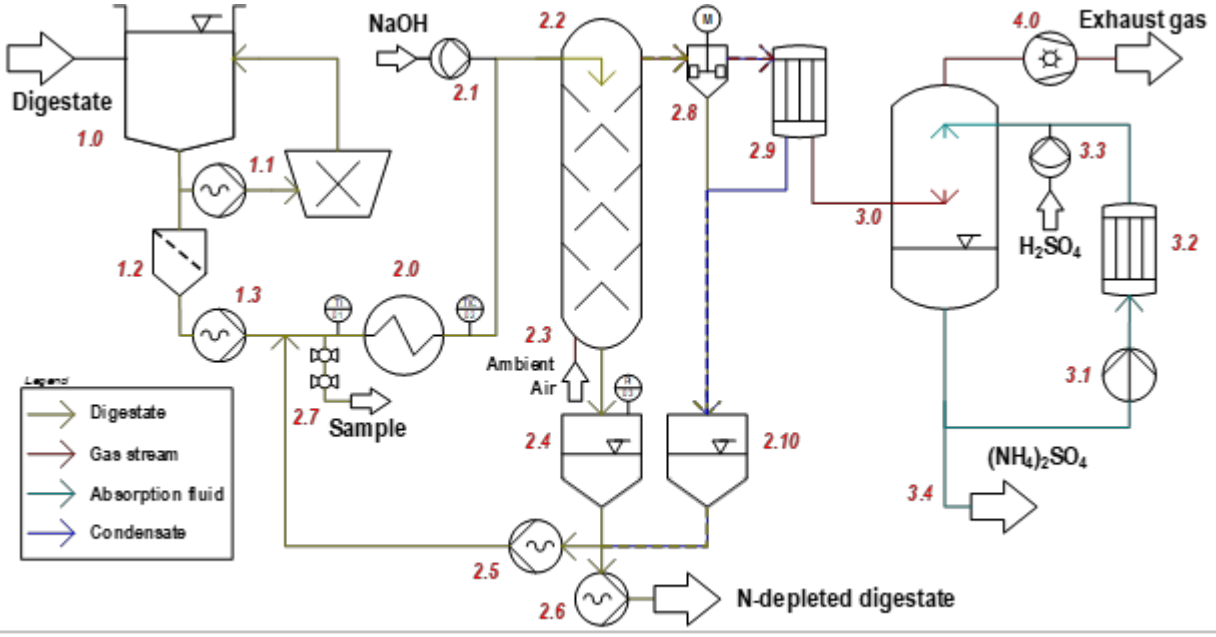

Figure 12: Process flowsheet of the pilot unit after construction

Figure 12 depicts a flowscheme with the most crucial aggregates. Flows like cooling water and additional EI&C measuring points that have not been used for analysis of test results are not included to improve readibility.

The storage vessel **1.0** is filled with liquid digestate. Up to approx. 1 m^3 can be stored at a time for testing purposes. The eccentric screw pump **1.1** delivers the digestate into a macerator that is used to homogenize any remaining coarse contents like fibers. The processing is pumped back into the storage tank. A 3x15 mm slotted mechanical screen **1.2** is

used to further reduce the content of coarse contents and prevent potential clogging in the main system. Via eccentric screw pump **1.3** up to 150 L/h digestate are pumped into the main process.

Heat exchanger **2.0** warms the digestate to the desired temperature. The measuring points for the sample temperature TI01 and the temperature control/measuring point for the process temperature TIC02 are situated before and behind the heat exchanger. Sodium hydroxide can be added at **2.1** via a membrane pump. The centerpiece of the process is the degasification column **2.2**, where the digestate enters from the top and trickles down over alterating cones and funnels while ambient air (or the recycled exhaust gas; not shown) **2.3** is brought in contact in counterflow direction. Process digestate is collected in the column sump **2.4**, that in reality is directly situated under the processing column and not a separate vessel. At this place the process pressure is measured with PI03. To increase the hydraulic retention time of the digestate in the (continuous) process, an eccentric screw pump **2.5** recirculates the processed digestate back into the main loop while a smaller volume is drained with pump **2.6** and leaves the system as N-depleted digestate. The recirculated substrate enters before the heater so temperature losses can be compensated before entering the column again. The sample for analysis is taken at **2.7**. Note, that in batch tests the sample is not mixed with fresh digestate and thus representative for the experiment, while the sample in continuous mode has to be taken near the outlet of the plant. At the column head the gas NH_3-enriched gas stream leaves the column and enters a foam breaker **2.8** that reliquifies any built foam. Humidity in the gas stream is condensated by the tubular heat exchanger **2.9** (using regular tap water as a cooling agent). The fluid streams from both aggregates is united and flows into the collecting tank **2.10**, that feeds the collected fluid back into the main system via recirculation pump 2.5.

The enriched gas stream enters spray absorption **3.0**. Centrifugal pump **3.1** circulates the absorption fluid (design-wise sulphuric acid) over heat exchanger **3.2** that cools down the solution to enhance the absorption capability. Consumed sulphuric acid is refilled by membrane pump **3.3**. At **3.4** the reaction product di-ammonia sulphate can be drained.

Downstream of all the liquid ring vacuum pump **4.0** is used to create the necessary gas flow and reduce the pressure.

3.3. Desorption: Initial design

The initial design as displayed was tested using conditions derived from the laboratory experiments. Since the exact conditions (60 °C and 190 mbar p_{abs}) lead to spontaneous pump failure, the temperature was increased to 70 °C and the pressure to 310 mbar, to still use the boiling point of water as the working condition but fix the problem regarding the pumps [14]. The airflow and the associated gas-liquid-ratio was picked arbitrarily. The ratio is particular low, hence 150 L/h were recirculated with the recirculation pump.

The conducted tests are displayed in Table 6.

Table 6: Overview test series A (initial design); seven tests were carried out to identify the effects of different parameter sets (T, p, pH and V_G/V_L) on the process at pilot scale

ID	ϑ	p_{abs}	pH	Q_{air}	$(V_G/V_L)_{norm}$	Brief description
	[°C]	[mbar]	[-]	[m^3/h]	[L_N/L]	
A1	70	310	-	3	21	No NaOH added to see effect of carbonate buffer removal
A2	70	310	9	3	21	High T, low p, high airflow
A3	70	310	9	3	21	NaOH added after 60 mins of stripping at 800 mbar
A4	70	310	9	3	21	NaOH added after 30 mins of stripping at 800 mbar
A5	70	310	9	2	13	High T, low p, medium airflow
A6	70	310	9	0	0	High T, low p, no airflow
A7	35	310	9	3	21	Low T, high p, high airflow

In test A1 no NaOH was added to test the possibility of using the process to simultaneously remove CO_2 and see the effects on TAN removal. In A2 the reference pH of 9 was used. A3 and A4 are combinations of A1 and A2. For 60 respectively 30 minutes the process was operated at 800 mbar 70 °C to remove CO_2 and weaken the carbonate-

bicarbonate buffer system, after that NaOH was added to increase the pH to 9 and increase the share of FAN. The stripping gas stream was decreased in A5 to be able to quantify the impact. In A6 no gas stream was introduced into the process for the same reason. A7 was conducted to see the impact of the temperature at otherwise similar parameters to the most beneficial conditions in trial A2.

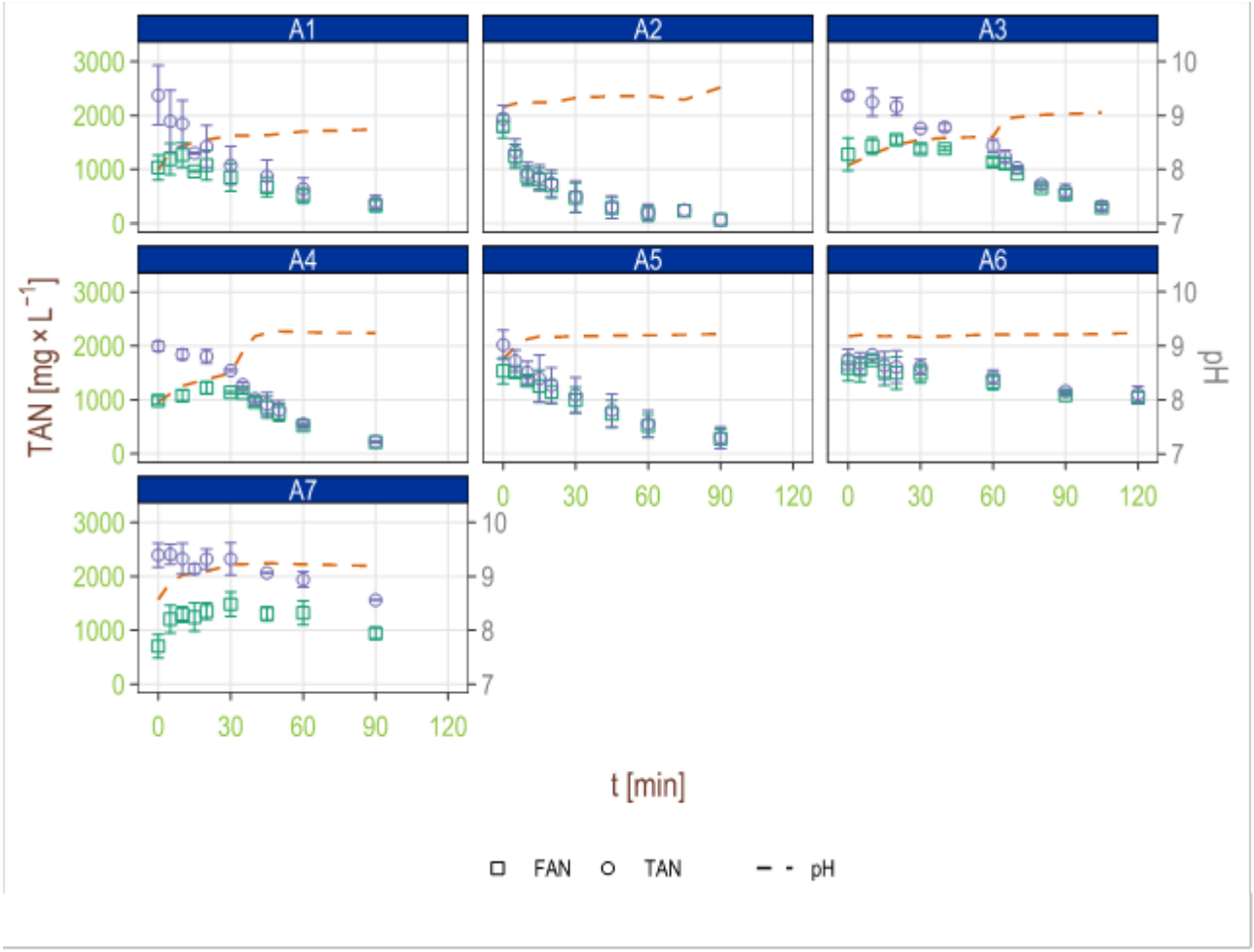

Figure 13: TAN and pH/temperature dependent FAN concentration of test series A in the conducted batch tests with mean pH

Table 7: Half-life of TAN at different process conditions in series A

ID	A1	A2	A3 (0-60 min)	A3 (60-90 min)	A4 (0-30 min)	A4 (30-90 min)	A5	A6	A7
ϑ [°C]	70	70	70	70	70	70	70	70	35
p [mbar]	310	310	800	310	800	310	310	310	310
pH	No adjust.	9	No adjust.	9	No adjust.	9	9	9	9
$(V_G/V_L)_{norm}$ [L_N/L]	21	21	21	21	21	21	13	0	21
t_{50} [min]	**36**	**22**	**85**	**21**	**138**	**22**	**34**	**168**	**155**

According to observations, the elimination in the batch process can be approximated by first order kinetics. The associated fit curves can be seen in the Annex (Annex I for series A). Derived from that, the half-life of the TAN concentration can be used as a comparative value. Strictly taken, the precision of this value only holds true for constant pH and temperature, since the FAN concentration - the fraction of removable N – changes with these parameters. The half-life of the series A tests are listed in Table 7.

The TAN concentrations for the batch tests in Series A are displayed in Figure 13. Comparing A1 and A2 the benefits of adjusting the pH becomes visible. Due to the higher FAN content from the start, A2 ends up with a higher elimination rate and reaches 50 % TAN_{elim} after 22 in comparison to 36 minutes. The second phase of A3 and A4 also reaches the same rate. The impact of CO2 removal on the pH is clearly visible in A1 and the first phases of A3 and A4, where no NaOH was added. The pH value could naturally be increased from around 8 to 8.8 in A1 and 8.5-8.8 in A3/A4 depending on time used for removing CO_2. Lowering or removing the stripping gas flow (A5/A6), the elimination rate decreases. With 2 m^3h^{-1} of air, t_{50} was 34 min instead of 22 in the reference test. Without air, it takes 168 min to remove 50 % of the TAN. Lowering the temperature from 70 °C to 35 °C (A7), the removal was also significantly slowed (t_{50} = 155 min).

In A2, 6 mL of $NaOH_{50\,\%}$ were used per L of digestate to initially increase the pH to around 9. After removing CO_2 for 60 mins in A3, this amount was reduced to 1.7 mL/L and after stripping for 30 mins (A4) the necessary amount was still significantly lower with 3.2 mL/L to reach a pH of 9.

While the elimination rates are promising it was shown by analysis of the DR that significant loss of water occures at the process conditions (Table 8). At constant temperature and pressure, a high G/L ratio that benefits mass transfer of ammonia negatively impacts the water loss.

Table 8: Hourly water loss in the series A batch tests at 70 °C/310 mbar and different G/L ratios

ϑ [°C]	**70**	**70**	**70**
p [mbar]	310	310	310
$(V_G/V_L)_{norm}$ [L_N/L]	21	13	0
Water loss [%/h]	12,7	10,2	4,5

Without introducing an ambient air flow, 4,5 % of the total water mass were lost in the process. 2 m^3_{norm}/h of external air increased the loss to 10.2 %/h and 3 m^3_{norm}/h to a mean of 12.7 %/h. Water in the gas stream could not be properly condensated by the installed cooler and poses potential problems at the absorption stage, because it will recondensate in the absorber and dilute the product. The TAN concentration in the collected condensate was found to be close to the concentration in the digestate at a given moment. The evaporation enthalpy also drains energy from the system, that has to be recovered within the boundaries of the desorption process to not negatively affect the energy balance. To approach this problem, different types of vapor deposition fixtures were tested in test series B.

Additionally, the cone-funnel installations inside the desorption column were found to overload the system hydraulically. Flooding occured in the column that lead to digestate leaving the column at the top and overwhelm the foam breaker. This will eventually lead to digestate entering the absorption stage. Even though the system was proposed to be able to treat unseparated digestate, it was found too challenging for the pilot setup. It was possible to use unseparated digestate as feedstock, but even after homogeniztation with the macerator and pre-separation at the mechanical screen, clogging still sporadically occured. This is partly due to the fact, that in contrast to industrial scale units, pipe diameters as small as 3/8" are installed.

3.4. Desorption: Free-fall column

Test series B was conducted to get a grip on the hydraulic and energetic problems identified in series A. The main goals were to quantify and decrease the loss of water in the batch tests while maintaining a high rate of N elimination [15]. To achieve that, combinations of the temperature and pH were chosen, that increase the share of the FAN. The stripping gas flow was increased to 5 m^3h^{-1} in the tests with pH 10 and 45 °C to counteract the performance losses due to the lower temperature. Again, the liquid load of the column was 150 L/h via the recirculation pump.

The parameter combinations are displayed in Table 9. Runs B1 to B3 were conducted at 70 °C and 310 mbar and pH 9 with a stripping air flow of 20 L_N/L. In B4 to B6 the temperature was lower with 45 °C and 310 mbar, moving away from boiling point conditions, but an increased pH of 10. The gas liquid ratio was 33 L_N/L. Different setups of fixtures for vapor deposition/separation were tested. Overall, six combinations of two of the fixtures (tubular heat exchanger, column with

cone built-ins for increased are for condensation and a gas cyclone) were tested. The fixtures were connected in line and the condensate was collected separately.

Table 9: Overview test series B (free fall column); six tests were carried out to identify the effects of two parameter sets on the process using an empty column with anti wall effect fixtures and additional aggregates to test steam separation

ID	ϑ	p_{abs}	pH	Q_{air}	$(V_G/V_L)_{norm}$	Brief description
	[°C]	[mbar]	[-]	[m³/h]	[L_N/L]	
B1	70	310	9	3	20	Vapor deposition: (1) tubular heat exchanger + (3) gas cyclone
B2	70	310	9	3	20	Vapor deposition: (1) tubular heat exchanger + (2) column with cone built-ins
B3	70	310	9	3	20	Vapor deposition: (2) column with cone built-ins + (1) tubular heat exchanger
B4	45	310	10	5	33	Vapor deposition: (1) tubular heat exchanger + (3) gas cyclone
B5	45	310	10	5	33	Vapor deposition: (1) tubular heat exchanger + (2) column with cone built-ins
B6	45	310	10	5	33	Vapor deposition: (2) column with cone built-ins + (1) tubular heat exchanger

The changes to the plant setup for series B are shown in Figure 15. Instead of alterating funnels and cones that led to flooding of the column due to a cross section reduction by 91 %, the column was redesigned to contact the counterflow of stripping gas in free fall. Rings were installed on the inside of the column to lead any digestate that flows on the inner wall back into the free area and increase the specific contact area. The cross section reduction was reduced from 91 % to 19 % this way. The fixtures are schematically shown numbered (1) to (3). The tubular heat exchanger **(1)** from the initial design was reused in this scenario. Parts of the old column were repurposed to see a possible effect of the redirection of the gas stream through the alternating cones and funnels and test the vapor deposition **(2)**. Finally, a gas cyclone was installed to see the effect of separation through centripetal forces introduced by the velocity of the gas stream **(3)**.

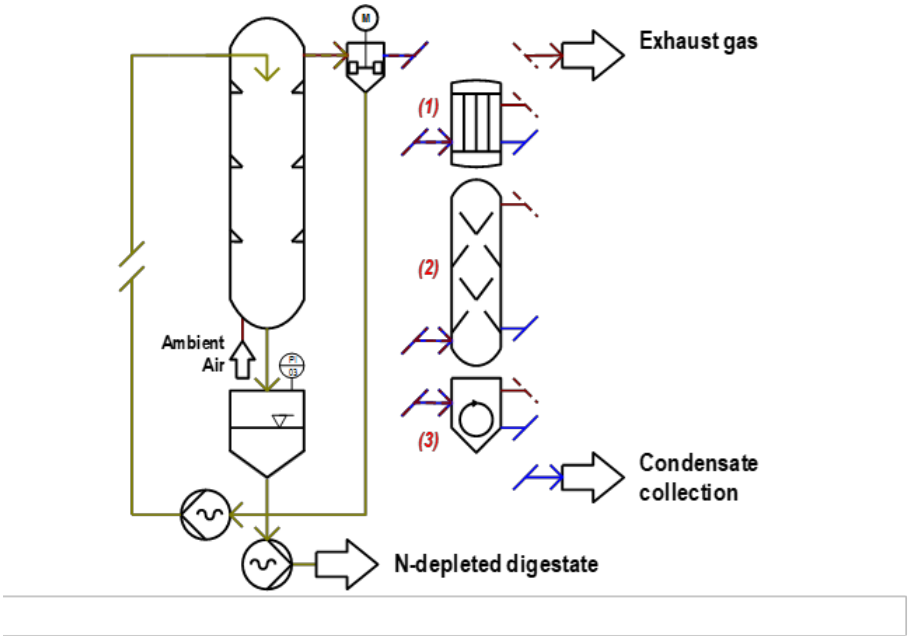

Figure 14: Modified column with anti wall-effect rings and fixtures tested in series B to separate steam from the gas flow; (1) tubular heat exchanger, (2) column with cone built-ins, (3) gas cyclone

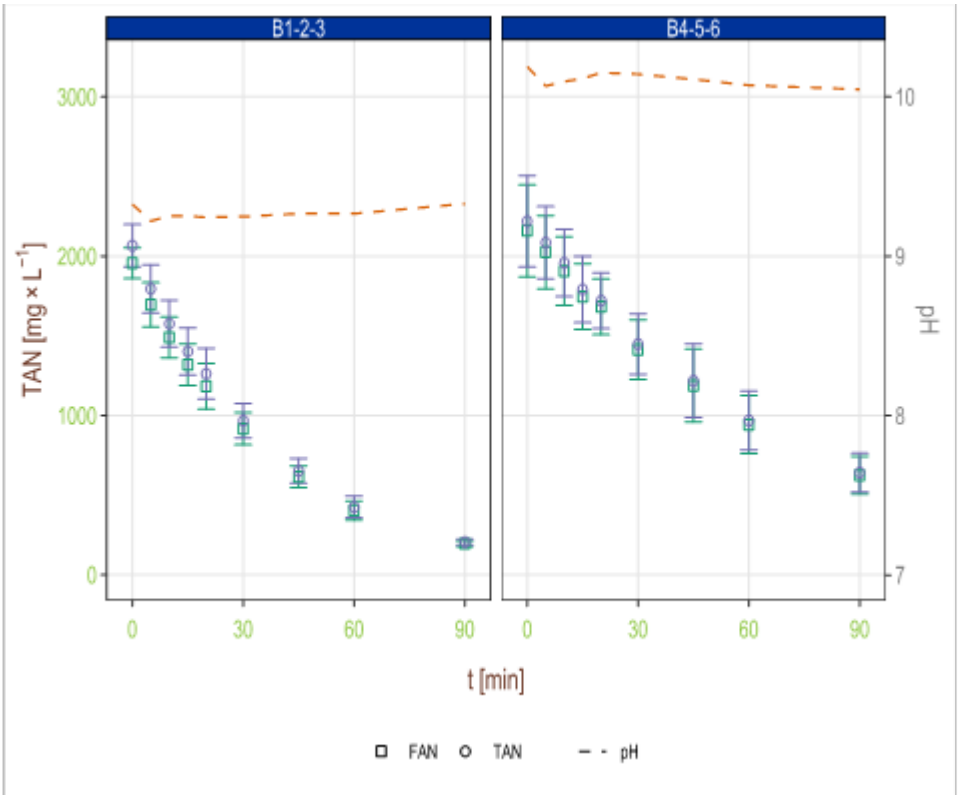

Figure 15: TAN and pH/temperature dependent FAN concentration of test series B in the conducted batch tests with mean pH

In regard to the elimination of ammonia, tests B1 to B3 and B4 to B6 can be summarized since they share similar process conditions. Figure 15 displays the progressions of TAN, FAN and pH over the duration of the batch tests. While the FAN concentration share is approximately equal in both trials (Figure 15), the time to reach 50 % TAN eliminated is 27 min in the tests with 70 °C and pH 9 (real mean pH slightly higher than targeted) but 50 min in the 45 °C and pH 10 tests. The greater specific stripping gas volume flow was not sufficient to counteract the process slowdown due to the low temperature condition (Table 10).

Table 10: Half-life of TAN at different process conditions in series B

ID	B1-B3	B4-B6
ϑ [°C]	70	45
p [mbar]	310	310
pH	9	10
$(V_G/V_L)_{norm}$ [L_N/L]	20	33
t_{50} [min]	27	50

Regarding the evaporation of water, the water loss per hour is comparable to the results of series A. If at all, the different column geometry in series B aggravates the water loss at high temperatures with an hourly loss of 12.8 %. The reduction in temperature to 45 °C with an elevated stripping gas stream of 33 L/L significantly reduces the loss to a mean of 4.1 % per hour. The best tested setup for steam condensation was a combination of the tubular heat exchanger and gas cyclone. Still, only 11.6-14.6 % of the evaporated water in the gas stream could be recovered by the fixtures. A lower overall temperature does not seem to have an effect on the total amount recovered relative to the water content in the gas stream. Therefore, more efficient means have to be implemented to keep the elimination of ammonia high but limit the amount of evaporated water (or increase the recovery of steam).

Table 11: Hourly average water loss in the series B batch tests

ϑ [°C]	**70**	**45**
p [mbar]	310	310
$(V_G/V_L)_{norm}$ [L_N/L]	20	33
Water loss [%/h]	15	4.1
Water recovered [%/h]	2.2	0.5
Net water loss [%/h]	12.8	3.6

3.5. Desorption: Packed column

Using the cognitions won in series B, the column was redesigned once again to feature packing [16-18]. Packing material is used to enlarge the surface area of the fluid to be treated and provide opportunity for phase transfer to happen. The desorption stage of the test series in schematically shown in Figure 16. Even though thermal energy was identified as the main driver of the process kinetics, the temperature was set to 45 °C in this series to prevent excessive water evaporation. To compensate for the lower FAN share, pH was increased to 10. Three different types of packing material were tested: two 15 mm high-flow type rings (ENVIMAC and RVT) and one 1" ring with low pressure loss (NSW NOR-PAC). The packings were tested in C2-C4. C6 did not use any packing, instead the column was as in series B. C1 and C7 were conducted to test the influence of temperature or pressure changes in combination with a high performance column geometry. The influence of two-stage packing was tested in C5. For series D, 5 L of RVT Hiflow type 15 mm rings were used as packing material in all tests. Main objective of the tests was the commissioning of the scrubbing unit. Regarding desorption, different sets of parameters were tested/repeated. In tests where NaOH was used, CO_2 was removed for 30 mins at the same temperature/pressure and airflow levels before dosing base. To see the effect, CO_2 levels in the digestate of series D were analyzed photometrically as well as TAN levels. The parameters for both series using packing can be found in Table 12. Also, a recirculation rate of 150 L/h was used

Table 12: Overview of test series C and D (packed column); different packings were tested in series C to see the effect on the degasification efficiency, the parameter sets were varied in series D to see possible effects on the process and test the most suitable setup for downstream absorption

ID	**ϑ**	**p_{abs}**	**pH**	**Q_{air}**	**$(V_G/V_L)_{norm}$**	**Brief description**
	[°C]	**[mbar]**	**[-]**	**[m^3/h]**	**[L_N/L]**	
C1	45	310	-	5	33	Packing: ENVIMAC Hiflow 15 mm 5 L
C2	45	310	10	5	33	Packing: ENVIMAC Hiflow 15 mm 5 L
C3	45	310	10	5	33	Packing: NOR-PAC NSW 5 L
C4	45	310	10	5	33	Packing: RVT Hiflow 15 mm 5 L
C5	45	310	10	5	33	Packing: ENVIMAC Hiflow 15 mm 4.6 L intermediary with fluid redistribution
C6	45	310	10	5	33	No packing; reference
C7	45	800	10	5	33	Packing: ENVIMAC Hiflow 15 mm 5 L
D1	65	500	-	5	33	Packing: RVT Hiflow 15 mm 5 L; no NaOH added
D2	65	500	9	5	33	Packing: RVT Hiflow 15 mm 5 L; NaOH added after 30 mins of stripping at 500 mbar
D3	65	500	9	2.5	17	Packing: RVT Hiflow 15 mm 5 L; NaOH added after 30 mins of stripping at 500 mbar
D4	65	500	9	0	0	Packing: RVT Hiflow 15 mm 5 L; NaOH added after 30 mins of stripping at 500 mbar
D5	65	800	9	5	33	Packing: RVT Hiflow 15 mm 5 L; NaOH added after 30 mins of stripping at 800 mbar
D6	45	500	10	5	33	Packing: RVT Hiflow 15 mm 5 L; NaOH added after 30 mins of stripping at 500 mbar
D7	45	800	10	5	33	Packing: RVT Hiflow 15 mm 5 L; NaOH added after 30 mins of stripping at 800 mbar

The desorption section flow scheme for series C and D is shown in Figure 16. Additionally to the adaption of the internal column geometry, the cooling capacity of the tubular heat exchanger was enhanced by allowing a higher volume flow of cooling water. Condensate is no longer separately collected but instead led back to the recirculation loop. At the given process conditions it takes 52 min to remove 50 % of the TAN in the reference test of series C (C6). Using packing by ENVIMAC and RVT (C2/C4), this time decreases to 34 respectively 42 min. Since the mean pH in C4 was too low by approx half a unit, there shouldnt be any significant difference between the two tests. Both packing types overall share comparable to similar dimensions. The larger packing by NOR had a longer time to remove hald of the TAN compared to the reference test, but was also undershot pH wise, so that a neutral impact by this packing type could be determined. C1 shows that without pH adjustment 45 °C is not enough to raise the FAN content enough in the proposed system design. t_{50} is 181 min, considerably longer in comparison to the high temperture test without pH adjustment A1 (36 min). Using a 2-step packing with a 1 cm sieve-plate for fluid redistribution in between (C5), did not yield a different result than the 1-step packing with the same fill material. A pressure of 800 mbar instead of 500 at otherwise similar conditions more than doubled the degasification time for t_{50}. An overview over the process conditions and the associated half-life times can be found in Table 13. The FAN/TAN measured values and pH over time are shown in Figure 17. Regarding the DR, 5.1 % of the water were lost on average at 45 °C/310 mbar and G/L = 143 L (Table 14) with the adjusted cooling water flow. At higher pressure (800 mbar), this could be reduced to 1.1 %.

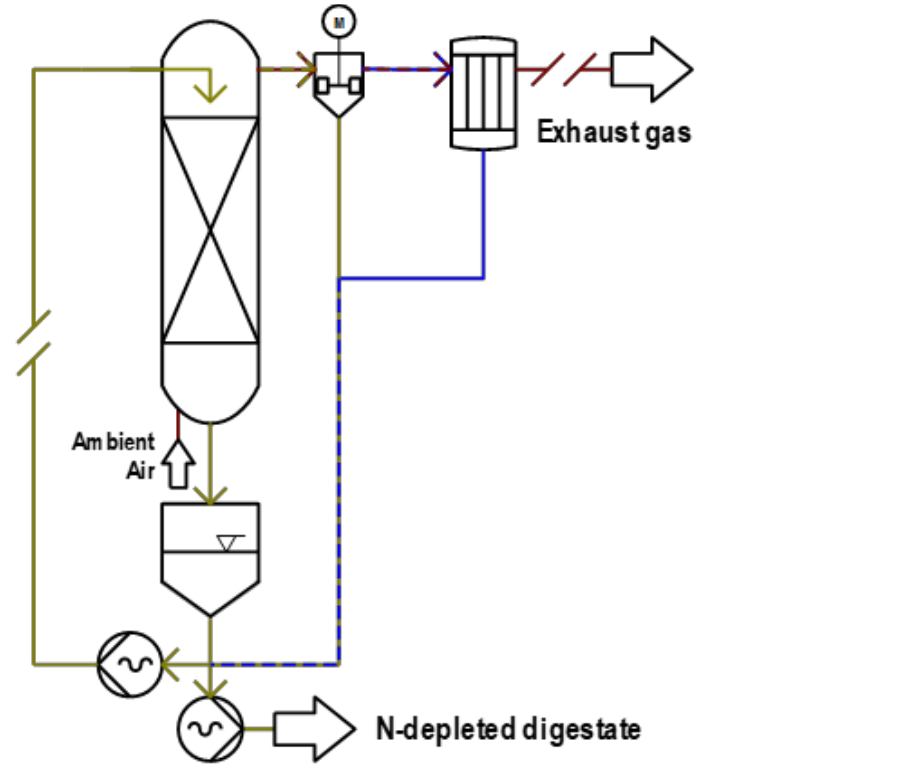

Figure 16: Packed column used in test series C and D; the condensate is no longer collected for quantification

Table 13: Half-life of TAN at different process conditions in series C

ID	C1	C2	C3	C4	C5	C6	C7
ϑ [°C]	45	45	45	45	45	45	45
p [mbar]	310	310	310	310	310	310	800
pH adjust.	-	10	10	10	10	10	10
$(V_G/V_L)_{norm}$ [L_N/L]	33	33	33	33	33	33	33
Packing	ENVIMAC	ENVIMAC	NOR-PAC	RVT	ENVIMAC	-	ENVIMAC
t_{50} [min]	**181**	**34**	**61**	**42**	**34**	**52**	**93**

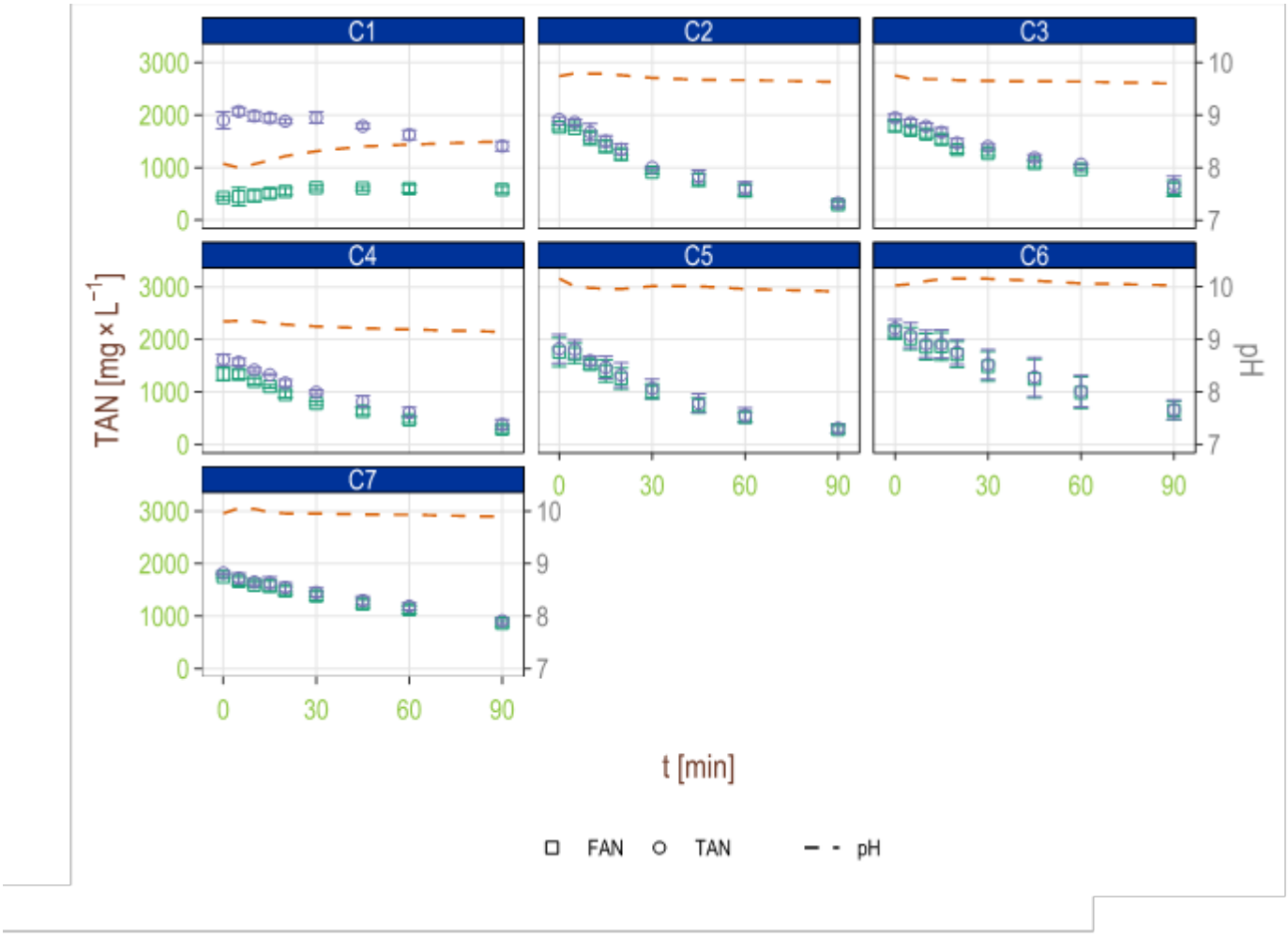

Figure 17: TAN and pH/temperature dependent FAN concentration of test series C in the conducted batch tests with mean pH

Table 14: Hourly average water loss in the series C batch tests

ϑ [°C]	**45**	**45**
p [mbar]	310	800
$(V_G/V_L)_{norm}$ [L_N/L]	33	33
Water loss [%/h]	**5.1**	**1.1**

Since series C yielded, that the RVT packing was suitable for the task, it was used in all tests of series D. Less samples were taken, since the kinetics were sufficiently studied in series A to C. In all tests where the pH was adjustet (D2 to D7), the batch was first processed for 30 min without added caustic soda to remove part of the carbonate buffer. Since 45 °C were found too low to efficiently remove ammonia, the temperature was arbitrarily set to 65 °C with a pressure of 500 mbar to counteract evaporation and be far enough away from boiling point conditions (which at this temperature would be 250 mbar). From the half-lifes (Table 15) it is apparent, that the elimination time after the partial removal of the carbonate buffer are increased threefold at the given process conditions in all tests where NaOH was added. The amount of NaOH needed for pH 9 was 2.25 g/L and for pH 10 6.75 g/L. In D2 to D4 the stripping gas flow was reduced from 143 L_{norm}/L via 71 to 0. Halving the gas flow led to more than double the averaged half-life. Without flow - as in earlier tests - the eliminaton was negligibly small. Variations of the pressure also had impact on the elimination rate. Compared to D2 in D5 where the absolute pressure was 800 mbar instead of 500, the half-lifes in both phases (unadjusted and adjusted pH)

roughly doubled. At 45 °C (D6 and D7) the higher absolute pressure also increased the half life after the addition of NaOH from 44 min to 79 min. Before adding NaOH no significant removal of TAN could be observed at 800 mbar p_{abs}.

Table 15: Half-life of TAN at different process conditions in series D

ID	D1	D2		D3		D4		D5		D6		D7	
t [min]	*0-60*	*0-30*	30-60	*0-30*	30-60	*0-30*	30-60	*0-30*	30-60	*0-30*	30-60	*0-30*	30-60
ϑ [°C]	65	65		65		65		65		45		45	
p [mbar]	500	500		500		500		800		500		800	
pH adjust.	-	-	9	-	9	-	9	-	9	-	10	-	10
$(V_G/V_L)_{norm}$ [L_N/L]	33	33		17		0		33		33		33	
t_{50} [min]	65	77	21	125	47	-	185	154	48	111	44	-	79

The concentration and pH progressions of series C and D are depicted in Figure 17 and Figure 18. It becomes visible, that at a low temperature of 45 °C (C1, D6/D7 0-30 min) the FAN share without adjustment of pH is very low and thus leads to a slow elimination rate regardless of other parameters. As in earlier series, the effect of higher temperature with otherwise similar parameters is apparent. Additionally to measuring the TAN in series D the carbonate concentration as CO_2 was measured at the start of the experiment, before adding NaOH at the 30 min mark and after 60 min (Figure 19). The corresponding values are outlined in Table 16. Discrepancies in the starting concentrations of the batch tests may be due to concentration changes in the storage process of the digestate. Tests were carried out over several weeks.

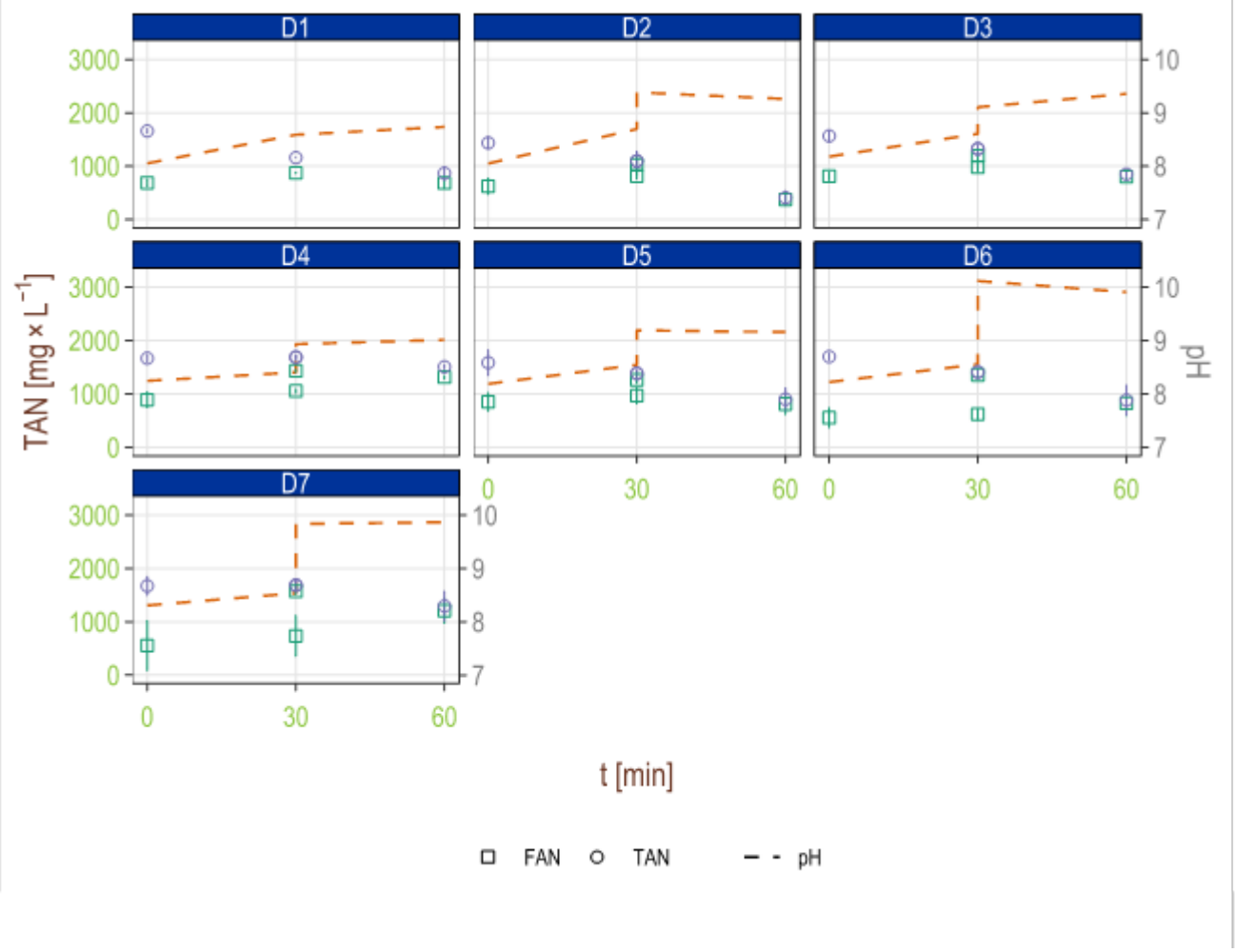

Figure 18: TAN and pH/temperature dependent FAN concentration of test series D in the conducted batch tests with mean pH

At average the largest quantity of CO_2 was removed in D1, where no NaOH was added after 60 min. This is expected, since adding NaOH shifts the balance of CO_2/HCO_3^- further to CO_3^{2-} which can't be stripped in gaseous form. 42.8 % of the carbonate buffer were eliminated in this test, with 24.9 % being eliminated in the first 30 mins. Adding NaOH after 30 min decreases CO_2 elimination in the second half of the experiment (D2) but overall only slightly lowers the removal to 39.9 %. Higher airflows were able to remove more CO2, but even just by thermic effect at 65 °C 23.9 % of the carbonate buffer were removed (D4). Lower overall temperature and higher absolute pressure both led to less CO_2 removal (D6/D7).

Table 16: Carbonate as CO_2 in series D, measured at the start of the experiments, before dosing NaOH at the 30 min mark and after 60 min and average relative elimination

	t [min]	D1	D2	D3	D4	D5	D6	D7
c_{CO2} [mg/L]	0	7967 ± 501	6983 ± 605	7200 ± 500	8300 ± 50	7150 ± 1418	7233 ± 236	7633 ± 275
	30	5983 ± 693	5140 ± 537	6233 ± 633	7367 ± 660	5800 ± 180	6733 ± 603	6967 ± 625
	60	4558 ± 488	4198 ± 972	5118 ± 598	6317 ± 813	5132 ± 254	6117 ± 791	6767 ± 861
$\%_{elim}$	0-30	24.9	26.4	13.4	11.2	18.9	6.9	8.7
	30-60	23.8	18.3	17.9	14.3	11.5	9.2	2.9
	0-60	42.8	39.9	28.9	23.9	28.2	15.4	11.4

In D3, D4 and D6 the mean relative loss of CO_2 was greater after adding the NaOH, which is likely explained by the range of the deviations. Overall the removal of CO_2 still seems to work at pH 9 and higher at the proposed parameters, but adding NaOH sooner increases the efficiency of TAN removal as sufficiently shown.

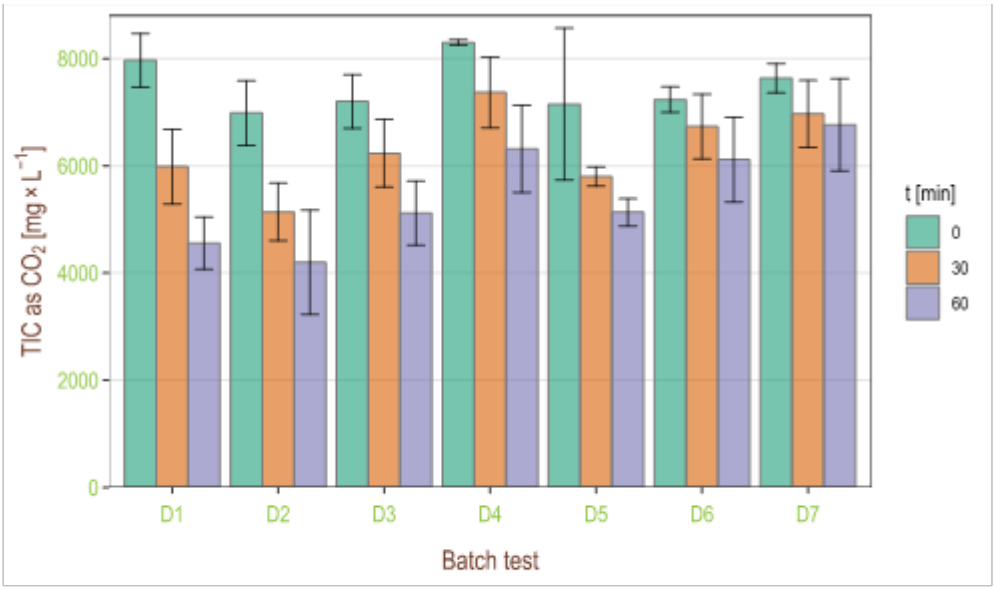

Figure 19: TIC as CO_2 in the series D batch tests

3.6. Absorption

Commissioning of the initial absorption column was conducted during series D [17]. The flow scheme of the column is shown in Figure 20. The entry point of the gas was realised severly high within the column. The absorption liquid is circulated with a pump with a volume flow of 1.3 m³/h, cooled and sprayed via a spray absorption into the absorption column. The dosage of sulfuric acid was not realised and manually dosed once during the batch trail. Due to the neglegible contact area as a result of the high gas entry of the column, the estimated recovery rates are comparably low.

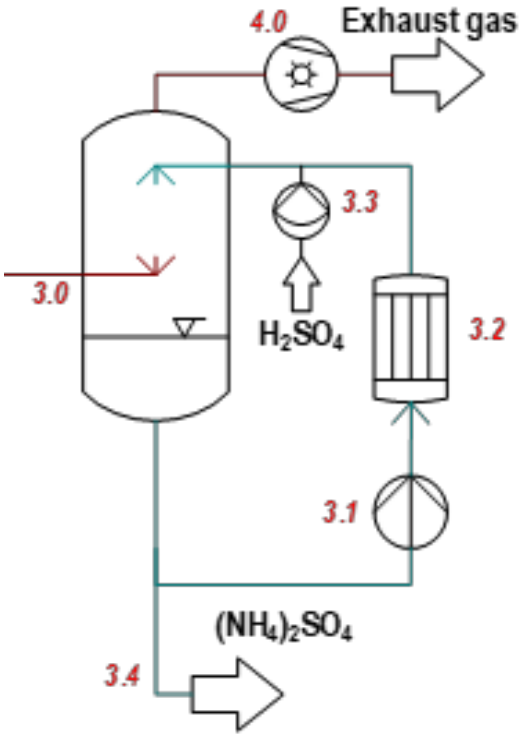

Figure 20: Scrubber design during commissioning phase

In terms of balancing the absorption column several limitations are given:

- The desorption column during the operation was operated discontinously, meaning that y_{in} (**3.0**) is not constant over the time of experiments. It can be assumed, that y_{in} (TAN) is moderate in the beginning due to the high gradient and "low" pH value, as the pH-value increases during CO_2 stripping and the gradient declines during simultaneously NH_3 stripping. After addition of caustic soda after 30 min the y_{in} (TAN) increases significantly and is then significantly reduced due to the quickly declining gradient and the low residual TAN in the substrate. In terms of y_{in} of CO_2, it can be assumed that it is high in the beginning due to the high gradient and "low" pH value and then decreases exponentially with the increasing pH and lower gradient, especially after NaOH is added. This is illustrated in Figure 21. To simplify the mass balancing to assess the efficiency of the absorption column a mean over $\bar{y}_{in}$ is calculated.
- The absorption column was operated also discontinously: on the one hand water was used to absorp NH_3 and CO_2 and therefore the concentration of both species increases over the run-time of the absorption column, resulting in changes of the operation line of the absorption column. Secondly due to sorption of the weak acid CO_2 and the medium base NH_3 the pH-value increased over the absorptions column runtime, resulting in different $\gamma_{A/B}$ and changes of the equilibrium line. Both factors leading in an increasing of the stripping factor S for NH_3 and therefore towards unfavourable sorption conditions for NH_3.

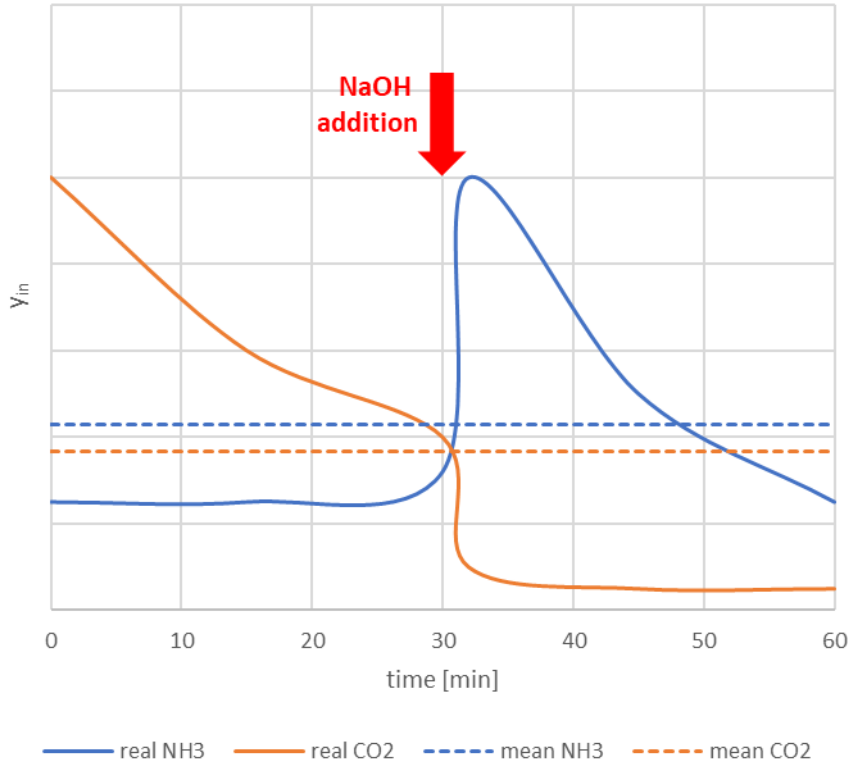

Figure 21: Schematic illustration of y_{in} of NH_3 and CO_2 and mean used for balancing the absorption column

Aware of these limitations, mass balances had been derived from the desorption performance to calculate the mass flow in the incoming gas flow $\overline{m}_{y_{in}}$. For a certain experiment, the initial mass flow $\overline{m}_{x_{in}}$ of the absorption liquid and the resulting mass flow $\overline{m}_{x_{out}}$ of the absorption liquid are given. The resulting mass flow $\overline{m}_{y_{out}}$ describes the mass flow in exhaust air. The calculated masses for $\overline{m}_{x_{out}}$ and $\overline{m}_{x_{in}}$ based on the measured concentrations and the desorption and absorption column batch volume are shown in Figure 22-

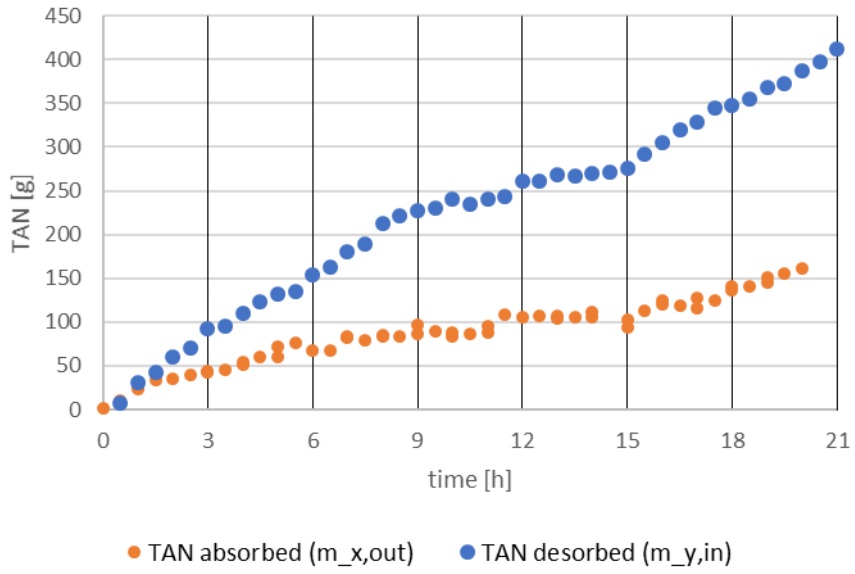

Figure 22: absoulte mass of TAN desorbed and absorbed during test series D, over the seven experiments, with 3 h run & repetition time of each experiment

The recovery rate in the absorption column is simplified defined in eq. 8. For each run of series D a seperate recovery rate had been calculated witch is shown in Table 17.

$$r_a = \left(\frac{\overline{m}_{x_{out}} - \overline{m}_{x_{in}}}{\overline{m}_{y_{in}}}\right)_a = \frac{\left(\overline{m}_{x_{out}} - \overline{m}_{x_{in}}\right)_a}{\left(\overline{m}_{x_{in}} - \overline{m}_{x_{out}}\right)_d} \quad \text{eq. 8}$$

r_a	Recovery rate for absorption	%
$\left(\overline{m}_{x_{out}} - \overline{m}_{x_{in}}\right)_a$	Mass increase of TAN/TCO_3 in the absorption column	kg
$\left(\overline{m}_{x_{in}} - \overline{m}_{x_{out}}\right)_d$	Mass decrease of TAN/TCO_3 in the desorption column	kg

Table 17: Recovery rates in the absorption column for series D

ID	D1	D2	D3	D4	D5	D6	D7
p [mbar]	500	500	500	500	800	500	800
$(V_G/V_L)_{norm}$ [L_N/L]	3.8	3.8	1.9	0	3.8	3.8	3.8
t_{50} [min]	43%	44%	64%	0%	42%	40%	38%

As illustrated in Table 17, the relation of gas volume flow and washwater is decicive for the recovery rate. Alos the gas load has sever effects on the recovery rate. All recovery rates had been comparably low, due to the low exchange space and neglegible specific surface area of the spray adsorption. The dosage of acid, reducing the activity of ammonia did not had any effects on the recovery rate. As a result the gas inlet was set to the bottom of the reactor and the adsorption column was filled with packings to increase the specific surface area to achieve multiple theoretical steps and therefore increase the recovery rate. It is then expect that a sufficient recovery degree can be achieved although the gas-liquid-ratio is higher. In fact also the absolute pressure has significant impact on the recovery rate especially of the volatile CO_2. With increasing absolute pressure, the gradient of the equilibrium line favours absorption as the Stripping factor S decreases.

3.7. Identified challenges and derivation of optimal operation parameters

The conducted test led to a multitude of findings that subsequently are going to be used to optimize the pilot process via the improved knowledge acquired. Regarding operation parameters it was shown, that the balance between temperature, pH value and volume flow of the stripping gas are crucial. The temperature is the most important factor in the process, since it impacts both the volatility of ammonia as well as the equilibrium between ammonium and ammonia. Since the acidic CO_2 is also effected by the solubility reduction at high temperature it is easier to remove it, this means that running the process at temperatures 65 °C or higher also reduces the amount of the caustic soda needed to adjust the pH. Regarding the influence on the buffer system, lower temperature means less removal of CO_2. Since a higher pH is needed to begin with, the amount of NaOH needed to reach the desired pH is negatively impacted by that additionally. Overall, analogous to the removal of TAN, CO_2 stripping was most impacted by the effect of high temperature. During the operation history of the VD for N-Recovery several observations could been identified limiting the plant capacity, which were adressed in the final pilot design:

- **Batch operations with recirculation:** The 35 L batch volume was operated with a recirculation volume flow of the liquid of 150 L/h, whereby 3-5 m³/h gas volume flow where used in counterflow. The $(V_G/V_L)_{norm}$ ratio was with 20-34 significantly to low. The column were operated with different Temperature and pH conditions at an absolute pressure of 0.3, 0.5 or 0.8 mbar. Although the low absolute pressure increased the gradient of the equilibrium line, the operationen line intersected the equilibrium line, due to the unfavourable gas-liquid ratio.

Consequently only low recovery degrees could achieved within one column throughput and the entire height of the column (of about 60-80 cm) could not been utilised with these process conditions. Furthermore the continuous reduction of the influent liquid gradient during the operation resulted in further dilution of the gas stream in terms of ammonia and a constant steam content due to ongoing evaporation of water. Additional batch operation of the desorption column were leading to discontinous gas loads entering the absorption column, whereby the derivation of a mass balance for the absorption column can only be realised with very rough estimations. To optimise the absorption column, constant gas loads are required which results in a continous operation of the desorption column.

- **Column design:** In conjuction with the small diameter of cones and funnels the high column loading, this led to column floding. Also an extensive packing at the liquid entry related to column flow. A moderate packing rate distinguished from the liquid entry and free-fall experiments resulted in very stable operations. However packings related to particle retention in the column, whereby the maximal operation duration before flodding due to particle clogging remains unknown. In terms of the absorption column, the spray absorption with limited contact area between gas stream and sprayed liquid led to recovery rates less than expected. Therefore the column design was changed, setting the gas inlet ot the bottom of the column and introducing packings, to run the absorption column similar to the desorption column.
- **Operational parameters:** As illustrated temperature, pH-value, absolute pressure and gas-liquid ratio are the crucial parameters on the operational performance. Temperature effects gas solubility and equilibrium between ion and soluble gas and evaporation of water while the gas-liquid ratio effects gas velocitiy and the equlibrium regarding degasification and evaporation due to convective transport of desorpt gases and steam. Meanwhile pH only influences the equilibirum between ion and soluble gas and absolute pressure effects the gas velocity, the gas solubility and evaportation. Conditions near to vapour conditions, lead to unfavorable heat and water loss and the pumps were not easily operatable near vapour conditions.

The main process parameters are chosen to maintain good stripping conditions, to reduce water losses and to maintain heat in the desorption column. Therefore the column is designed to operate with 0.9 mbar at a temperature of 70 °C with an $(V_G/V_L)_{norm}$ of 250 L/L. Due to simultaneous CO_2 stripping the pH increases towards an equilibrium of ammonia and carbon dioxide towards an estimated pH of approximately pH 9. No caustic soda should be applied. The aim is to recover about 95 % of ammonium and about 35 % of carbon dioxide.

In term of the thermic conditions, it is targeted that cold substrate enters and leaves the stripping column. Dry air is entering the column at its bottom and will be due to the conditions of 0.9 mbar and 70 °C saturated with steam. Due to steam generation a certain heat quantity is consumed related to the specific heat needed for water evaporation. This extracted heat reduces the temperature in the liquid towards a temperature of approximately 15 °C. The energy is transfered via the steam to the top of the column, where the steam saturated air gets in contact with the incoming cold substrate and the steam is recovered and consequently the heat gained by steam condensation will increase the temperature of the liquid towards the targeted column temperature of 70 °C. Heat losses can be regulated by an increase of the $(V_G/V_L)_{norm}$ or lowering the absolute pressure.

Within the scrubbing column ammonia and carbon dioxide are scrubbed with at a scrubbing temperature of 10 °C with a $(V_G/V_L)_{norm}$ of 165-170 L/L at 0.9 mbar with an pH-value of pH 7, so 99 % of the ammonia is recovered as ammonium and about 35 % of carbon dioxide is recovered as carbonate in the high loaded ammonium sulfate scrubber water. The pH increases during absorption, however through addition of gypsum and precipitation of limestone, the pH is neutralised to pH 7, hence the base carbonate is removed.

$$2\,NH_{3(aq)} + CO_{2(aq)} + CaSO_4 \cdot 2H_2O \leftrightarrow 2\,{NH_4}^+ + {SO_4}^{2-} + H_2O + CaCO_3 \downarrow \qquad \text{eq. 9}$$

The pumps for the substrate are equiped for a volume flow of 50-150 L/h. The vacuum pump is equiped with for a gas flow of up to 100 m³/h under norm conditions. The scrubber pump is equiped for a scrubbing water volume of 500-1500 L/h. These boundary conditions had been taken into consideration. Furthermore the diameter of the packings was given with

15 mm minimum diameter. Taking into consideration, that ratio between diameter of packings and diameter of the column should be between 1:10 and 1:30, the column diameter had been set to 0.2 m.

The digestate has an ammonium nitrogen concentration of 2 g/L and a total carbonate concentration of 10 g/L. Assuming a recovery target of 80 % TAN in the desorption column and 90 % in the absorption column a recovery rate of 27 % TCO_3 in the desorption and 24 % in absorption column is necessary to achieve the necessary molar ratio of $n(NH_3):n(CO_2)$ below 2:1 for the formation of Ammoniumcarbonate to realise the reaction with gypsum. Considering a substrate volume flow of 100 L/h, the resulting gas volume 25 m³/h and a scrubbing water volume of 1000 L/h, the results of the calculation are shown in Table 18.

Table 18: Calculation results for 80 % N-recovery in the pilot plant

		Recovery rate	Stripping factor	Height of packing	Relative wet pressure loss	Diameter relation
		[%]	S [−]	$H_{fill}[cm]$	$\left(\frac{\Delta p}{H}\right)_{wet}\left[\frac{mbar}{m}\right]$	$\frac{d_{col}}{d_{fill}}$ [−]
Desorption	NH_3	80	1.15	31	0.11	13
	CO_2	27	1.30	35		
Absorption	NH_3	90	$1.35 \cdot 10^{-5}$	28	0.11	13
	CO_2	24	4.09	34		

The stripping factors for desorption S > 1 are favorable, as well as the S (NH_3) < 1 for absorption. However the absorption of CO_2 is limited due to the comparably low pH of 7 near the pK_A of CO_2 and the high Henry's law constant. The height of packings is with about 25-35 cm comparably low. The relative pressure loss is with 0.11 mbar/m very low, indicating higher volume flows could be treated with this column. The diameter relation is with 13 between 10 and 30 as recommended.

If higher recovery targets e.g. 95 % TAN recovery should be achieved, also a higher recovery rate in absorption is necessary (see Table 19). Consequently the recovery target for TCO_3 increases towards 30 % in desorption and absorption. Therefore a higher scrubbing water volume flow of 1250 L/h is necessary. The stripping factors for absorption decrease compared to Table 18 due to higher liquid volume flow. The necessary height of packings decreases for the moderate CO_2 recovery targets due to the higher volume flow in the scrubber and higher recovery rate in the scrubber affecting the necessary height in the stripper. Meanwhile the height of packings for TAN recovery increases by about factor 2 when the recovery rate is 15 % higher. The relative pressure loss in the absorption column increases slightly due to the higher liquid volume flow.

Table 19: Calculation results for 95 % N-Recovery in the pilot plant

		Recovery rate	Stripping factor	Height of packing	Relative wet pressure loss	Diameter relation
		[%]	S [−]	$H_{fill}[cm]$	$\left(\frac{\Delta p}{H}\right)_{wet}\left[\frac{mbar}{m}\right]$	$\frac{d_{col}}{d_{fill}}$ [−]
Desorption	NH_3	95	1.15	70	0,11	13
	CO_2	34	1.30	53		
Absorption	NH_3	99	$1.08 \cdot 10^{-5}$	62	0,11	13
	CO_2	30	3.28	40		

The height of packings should at least be multiplied with 1.3 safely achieve the targeted recovery rate. Also the pre-heating and cooling in the desorption column needs to be considered, hence the calculated height of packings represents thermal and pH-conditions that must be achieved first.

Based on these observations and consideration of the theoretical design paramters, the following final VD-Design was targeted (see Figure 1). Digestate is filled into the storage tanked and mixed via the screw pump **P0** (optional via a cutter) back into the feed tank and is filled via the screw pump **P1** into the column **C1**. The substrate entry into column **C1** is halfway up, distinguishing the column into a steam absorption part at the columns center and a residual steam condensation part at the top of the column. The pre-heated substrate is pumped via the screw pump **P2** and the heat exchanger into column **C2**.

After passing the column **C2** the substrate is pumped via the screw pump **P3** into the column **C3**. After passing the column **C3**, the substrate is pumped via the screw pump **P4** out of the pilot plant. The sampling points for the substrate are after each screw pump **P1, P2, P3** and **P4**.

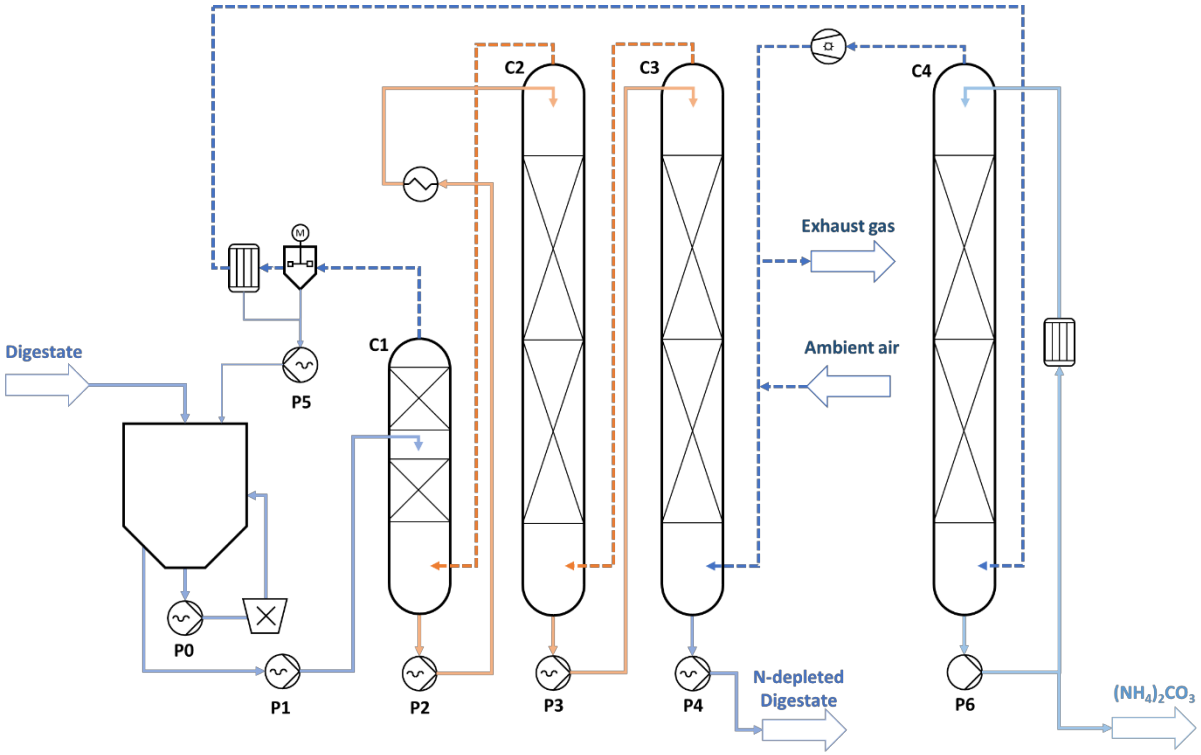

Figure 23: Flowscheme of the final VD-Design (heat conditions illustrated via colours: orange ≈ 70 °C; blue ≈ 15 °C)

Ambient air is suct in, in counter flow to the substrate. Ambient air is entering column **C3** and water evaporates at the columns bottom, while the substrate is cooled. The air containing the stripped gases and steam is suct via column **C2** into column **C1,** where the steam is condensing in contact with the cold substrate, resulting in pre-heating of the substrate. The air containing the stripped gases is cleaned via a foam breaker and condenser. Eventual condensate is pumped via **P5** back into the feed tank.

The high-loaded gas is the entering the absorption column **C4** and then recyceld via the vacuum pump. The absorption fluid is pumped back to the top of the absorption column via the pump **P6** and some of the absorption liquid is extracted as the recovered product or for sampling.

4. RECOMMENDATIONS FOR UPSCALING

These upscaling recommendations, are considering design guidelines, however no material properties for a long-lasting operation are considered. The desorption part, should easily be stable up to 80 °C for moderate pH-value (4-10). Therefore stainless steel is recommended, which should be thermally insulated. Also corrosion of both gases ammonia and carbon dioxide must be considered, so brass or materials containing copper should not be used, hence ammonia forms with copper complexes.

To operate the system with a tolerable pressure loss between 1-4 mbar/m, the column diameter and correspondingly the packings must be chosen. Under the described conditions (desorption: 0.9 bar, 70°C, pH 9 and an $(\dot{V}_G/\dot{V}_L)_{norm}$ of 250 L/L and absorption: 0.9 bar, 10°C, pH 7) an $(\dot{V}_G/\dot{V}_L)_{norm}$ of 20-25 is necessary to absorp the gases (especially a certain degree of carbon dioxide). If only ammonia recovery is targeted at low pH e.g. via dosage of sulfuric acid, the scrubber can be operated with a much higher $(\dot{V}_G/\dot{V}_L)_{norm}$ reducing the pressure loss. Figure 24 shows the column diameter in dependency from the volume flow of the substrate for desorption and absorption for 80 % ammonia recovery with an an $(\dot{V}_G/\dot{V}_L)_{norm}$ of 25 and for 95 % ammonia recovery with an $(\dot{V}_G/\dot{V}_L)_{norm}$ of 20. Hence the pressure loss increases with increasing water volume in the absorption stage, the column diameter increases for a fixed pressure loss of 2 mbar/m.

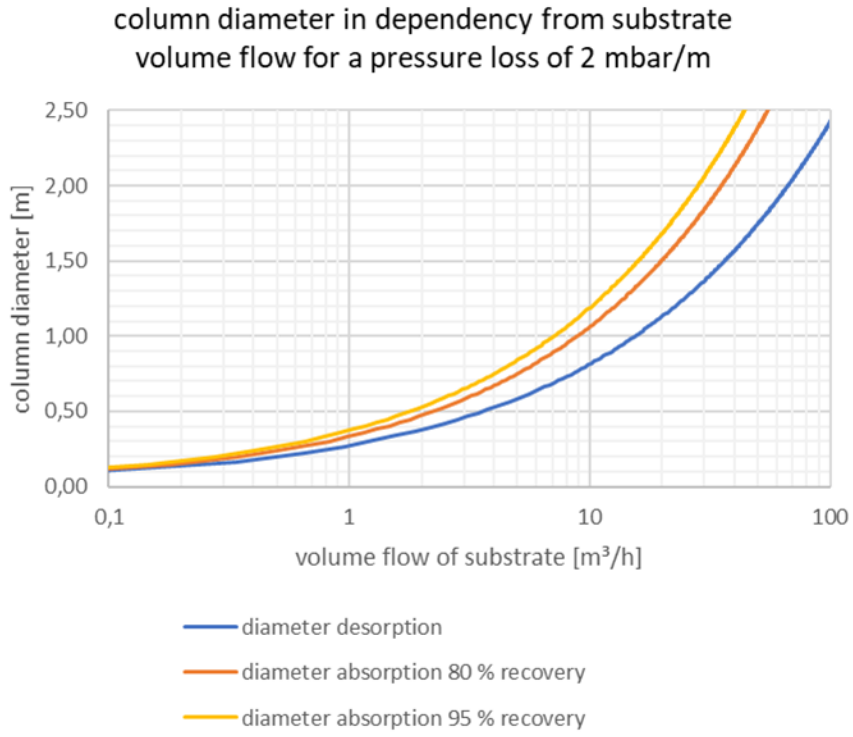

Figure 24: calculated column diameter for certain substrate volume flows minimizing the pressure loss towards to 2 mbar/m

The height of packings is linked mainly to the following parameters:

- The targeted recovery rate for ammonia
- The type, diameter and specific surface area of the packings and column

The diameter of the packings is resulting from the column diameter and should be at least 1 to 10 and maximum 1 to 30 to avoid so called maldistribution [11]. Consequently the diameter size of packings is also dependent from the volume flow. The calculated height of the packings for the described conditions (desorption: 0.9 bar, 70°C, pH 9 and an $(\dot{V}_G/\dot{V}_L)_{norm}$ of 250 L/L and absorption: 0.9 bar, 10°C, pH 7 and an $(\dot{V}_G/\dot{V}_L)_{norm}$ of 20-25 L/L) are shown in Figure 25. It became apparent that small packings with higher specific area, increase the overall surface area in the column an therefore reduce the column height. Depending on the volume flow of substrate, the column diameter and the diameter of packings are chosen and consequently different calculated height of packings must be adopted for a certain recovery rate. However in Figure

25 it becomes apparent that the column high significantly increases after a certain recovery rate of 80 % for large packings and of 95 % for small packings.

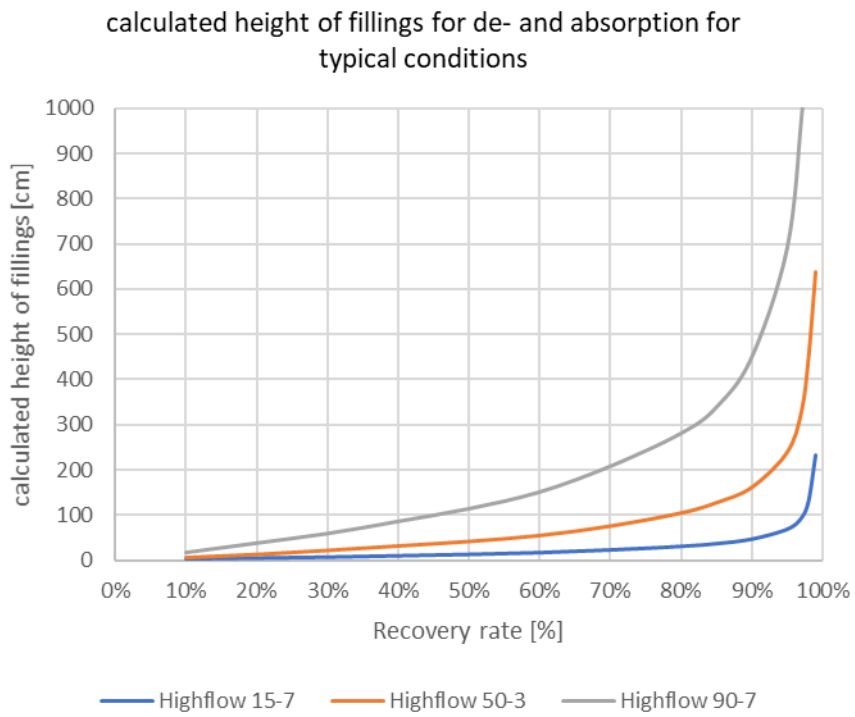

Figure 25: Calculated height of packings in dependency from the recovery rate for three different PP highflow packings with 15, 50 and 90 mm diameter

Two exemplary calculations had been performed for VD plants with a volume flow of 5 m³/h and with a volume flow of 20 m³/h for 80 % TAN recovery and 95 % TAN recovery each.

To realise an exceptable pressure loss for a volume flow of 5 m³/h a column diameter of 0.8 m is needed. Therefore larger packings are required to reach a diameter relation between 10 and 30. Here Highflow packings with 50 mm are chosen. Consequently a height of packings of up to 135 cm is calculated for 80% TAN recovery (see Table 20). The pressure loss is calculated with 0.26 mbar/m for the desorption column and 1.11 mbar/m for the absorption column.

Table 20: Calculation results for a column with a diameter of 0.8 m, a substrate volume flow of 5 m³/h and a target of 80 % TAN-Recovery

		Recovery rate	**Stripping factor**	**Height of packing**	**Relative wet pressure loss**	**Diameter relation**
		[%]	S [−]	$H_{fill}[cm]$	$\left(\frac{\Delta p}{H}\right)_{wet}\left[\frac{mbar}{m}\right]$	$\frac{d_{col}}{d_{fill}}$ [−]
Desorption	NH_3	80	1.15	106	0.26	16
	CO_2	27	1.30	118		
Absorption	NH_3	90	$1.35 \cdot 10^{-5}$	109	1.11	16
	CO_2	24	4.09	135		

If the TAN recovery rate is increased towards 95 % percent a height of packings of upt to 250 m is calculated. The pressure loss for the absorption stage increases towards 1.94 mbar/m hence the quantity of absorption water increases to achieve a high recovery rate in the scrubber (see Table 21).

Table 21: Calculation results for a column with a diameter of 0.8 m, a substrate volume flow of 5 m³/h and a target of 95 % TAN-Recovery

Recovery rate	**Stripping factor**	**Height of packing**	**Relative wet pressure loss**	**Diameter relation**
[%]	S [−]	$H_{fill}[cm]$	$\left(\frac{\Delta p}{H}\right)_{wet}\left[\frac{mbar}{m}\right]$	$\frac{d_{col}}{d_{fill}}$ [−]

Desorption	NH_3	95	1.15	238	0.26	16
	CO_2	34	1.30	181		
Absorption	NH_3	99	$1.08 \cdot 10^{-5}$	247	1.94	16
	CO_2	30	3.28	160		

For 20 m³/h substrate volume flow, a column diameter of 1.6 m is necessary to achieve a reasonable pressure loss. Again larger packings are chosen to realise the necessary diameter relation between column and packings to avoid maldistribution. The calculated height of packings is than up to 305 m for a TAN recovery rate of 80 %, while the pressure loss increases towards 1.32 mbar/m in the absorption column.

Table 22: Calculation results for a column with a diameter of 1.6 m, a substrate volume flow of 20 m³/h and a target of 80 % TAN-Recovery

		Recovery rate	**Stripping factor**	**Height of packing**	**Relative wet pressure loss**	**Diameter relation**
		$[\%]$	$S\ [-]$	$H_{fill}[cm]$	$\left(\frac{\Delta p}{H}\right)_{wet}\left[\frac{mbar}{m}\right]$	$\frac{d_{col}}{d_{fill}}\ [-]$
Desorption	NH_3	80	1,15	269	0,21	18
	CO_2	27	1,30	305		
Absorption	NH_3	90	$1,35 \cdot 10^{-5}$	292	1,32	18
	CO_2	24	4,09	249		

When the recovery target is again increased towards a recovery rate of 95 % TAN, the necessary height of packings increases towards up to 625 cm. The pressure loss in the absorption column increases towards higher quantity of absorption water needed towards 2.66 mbar/m (see Table 23).

Table 23: Calculation results for a column with a diameter of 1.6 m, a substrate volume flow of 20 m³/h and a target of 95 % TAN-Recovery

		Recovery rate	**Stripping factor**	**Height of packing**	**Relative wet pressure loss**	**Diameter relation**
		$[\%]$	$S\ [-]$	$H_{fill}[cm]$	$\left(\frac{\Delta p}{H}\right)_{wet}\left[\frac{mbar}{m}\right]$	$\frac{d_{col}}{d_{fill}}\ [-]$
Desorption	NH_3	95	1,15	619	0,21	18
	CO_2	34	1,30	465		
Absorption	NH_3	99	$1,08 \cdot 10^{-5}$	625	2,66	18
	CO_2	30	3,28	302		

As mentioned, The height of packings should at least be multiplied with 1.3 safely achieve the targeted recovery rate. Also the pre-heating and cooling in the desorption column needs to be considered in the design.

5. CONCLUSIONS

This chapter summarizes the thermodynamical and fluid dynamical basics related to the design of a VD plant. The following aspects can be summarized:

1. **Process conditions in the desorption stage and effects on water and heat:**
   - The relation of absolute pressure, temperature and volumetric gas-liquid-ratio in the desorption column, is not only crucial for ammonia recovery in the desorption stage but also for water and heat management.
   - With decreasing pressure, increasing temperature and increasing volumetric gas-liquid-ratio not only the removal efficiency of ammonia increases but also the unintended evaporation of water.
   - This leads to a) higher input of thermal energy and b) to water transfer and condensation into the absorbtion stage, diluting the ammonium sulfate product and also requires an efficient cooling of the absorption stage.
   - Hence steam is produced due to the conditions with lower absolute pressure than under norm conditions, high temperature and relevant gas-liquid-ratio, energy in form of heat is removed from the substrate resulting in low substrate temperatures at the column outflow.
   - This steam (containing energy) should be utilised to heat the cold substrate entering the column at the inflow resulting in heat recycling within the column. Also the incoming temperature of the substrate is thereby of importance for the exact process design.
   - The parameters (absolute pressure, temperature and gas-liquid-ratio) can be chosen in dependence from each other to optimise water, steam and heat management in terms to achieve a high ammonia recovery rate while minimizing the height of the packings in the column.

2. **Carbon dioxide and ammonia: buffers, pK_A-values and Henry's law constant:**
   - Agricultural digestate is a highly buffered system influenced by the buffer equilibria of ammonium and carbonate, with two sever buffers around pH 5-7.5 influenced by carbon dioxide/hydrogen carbonate and 8.5-11.5 by ammonium/ammonia and hydrogen carbonate/carbonate.
   - The pK_A constant of the acid-base system ammonium-ammonia is compared to other acid-base systems quite heavily influenced by temperature. Increasing temperature lowers the pK_A constant and also changes the buffers and pH.
   - Removing carbon dioxide via stripping from the digestate is a reaction consuming protons and is thereby increasing the pH ($HCO_3^- + H^+ \rightarrow CO_2 \uparrow$) . Meanwhile removing ammonia via stripping from the digestate is a reaction releasing protons and is thereby decreasing the pH ($NH_4^+ \rightarrow NH_3 \uparrow + H^+$). For an equilibrium of both reactions also Henry's law constant of both gases is relevant. For 70 °C, the equilibrium between both reactions is achieved around pH 9.2.
   - The temperature dependend Henry's law constant is decisive for the desorption. The Henry's law constant for ammonia is between 0.35 and 7.62 in the temperature frame of 10° C to 80° C. Meanwhile the Henry's law constant for carbon dioxide is between 1'040 and 5'470 in the same temperature frame. This means carbon dioxide is approximately by factor 1'000 more volatile than ammonia.
   - In terms of ammonia removal from the desorption stage, the effect of temperature is much more sever than the effect of pH-value. Not only the acid-base equilibrium is moved to ammonia, also the Henry's law constant significantly increases, such as the product out of activity coefficient and Henry's law constant.
   - Althought the conditions around pH 9 are not favorable for CO_2 stripping, hence CO_2 barely exists at pH 9, the high Henry's law constant off-sets this drawback, resulting in equal stripping efficiency compared to ammonia.

3. **Equilibrium and Operation line for De- and Absorption of Ammonia and Carbon dioxide**
   - The McCabe-Thiele Diagram describes the degree and the possibility of desorption or absorption. The equilibrium line is effected by Henry's law constant (influenced by temperature) and activity coefficient (influenced by temperature and pH value) and absolute pressure. The operation line is effected by gas-liquid-ratio and the recovery degree (influenced by the recovery rate and the initial loading of the gas/the liquid with the specific substance).

- The relation of gradients of the equilibrium and the operation line describes whether desorption or absorption is favored in the column. This is illustrated due to the stripping factor S describing the relation of gradients of both lines. A stripping factor superior than 1 favors desorption, while a stripping factor below 1 favors absorption. If this is not the case, equilibrium and operation line will cross each other, consequently the recovery is either impossible or only possible to a certain recovery degree.
- For constant operational parameters (absolute pressure, temperature, pH value and gas liquid-ratio) and a constant constructional parameters (column diameter and fittings) the necessary height equivalent of one theoretical plate HETP is also constant. This describes the height of packings until an equilibrium under given conditions is achieved. Recovery rate and/or recovery degree therefore influence only the number of theoretical plates ($NT_{d/a}$). The number of theoretical plates increases with increasing recovery rate and therefore the overall height of packings (H_{fill}) increases.

4. <u>Pressure loss in the desorption and absorption column and consequences</u>

- The pressure loss depends from several parameters, such as the column diameter, the packings and the gas and liquid load of the column. For low gas loads the pressure loss is constant and negligible. With increasing gas load, the corresponding liquid load becomes more relevant, hence friction and thereby the pressure loss is increased.
- Since a pressure loss towards 4 mbar/m is mentioned in the literature [11] as tolerable, the pressure loss increases towards a critical level when gas and liquid load are increased and the column diameter is kept constant. Consequently, the column diameter must increase with increasing substrate volume flow, to keep the pressure loss at a tolerable level.
- A ratio of packings diameter to column diameter of 1:10 to 1:30 is recommended, hence large packings in a column with small diameter leads to prefered liquid flow at the border of the column and small packings in a column with large diameter leads to maldistribution and preferencial flow of liquid and gas. Consequently with increasing substrate volume flow and increasing column diameter, the packings to be chosen for the column will increase in diameter.
- Increase in packing diameter is accompansied with a lower specific surface area and reduced bulk density. Consequently, the molar exchange is lower between liquid and gas phase for a certain height of packings and the height of packings increases compared to smaler packings.

5. <u>Overall process design, operational expenses and reliability compared to other state-of-the-art solutions</u>

- In terms of substrate composition and process stability, it is worth mentioning that stripping processes such as conventional air stripping and vacuum degasification are more tolerable towards higher DM-ratios and particles compared to membrane or IEX processes. However the process stability strongly depends on the column packings and their specific parameters. Adopting the process towards perforated plates, a lower specific exchange area and theirby lower recovery rate for the same column height is associated with higher toleration towards particles and the probability for clogging is reduced.
- Membrane or IEX process are adventageous in terms of space requirement, while conventional air stripping and vacuum degsification require higher columns depending on capacity and recovery rate. In terms of consumable, mainly electricity, heat, caustics and scrubber acids are of importance. In terms of electricity consumption the technologies varry with a specific electricity consumption of 1-2 kWh/m³ substrate. Heat consumption and caustic soda operation is mainly dependent on the operational conditions (high pH, moderate temperature vs. moderate pH, high temperature). In terms of heat, it is thereby of importance whether, how and with which efficiency heat can be recovered from the desorption effluent towards the influent. Normally the heat consumption is after heat recovery still about 5-10 kWh_{th}/m³ substrate, which is equivalent to a temperature deficit of about 5-10 K. In terms of pH, preceeding CO_2 stripping may effectively reduce the caustic soda consumption. The consumption of $NaOH_{50\%}$ is normally between 0-6 kg/m³ substrate. The challenges thereby are to reduce the heat deficit and operate the process without caustic soda. Within this study, it has been shown, that vacuum degasification is able to achieve this conditions, while maintaining a sufficient desorption. In terms of the absorption acid, the

consumption is dependent from NH_3 recovered and is for $H_2SO_{496\%}$ about 3-6 kg/m³ or alternatively to use about 6-12 kg gypsum/m³ as alternative sulfate source. In terms of economic and environmental costs, gypsum is preferred, also due to the formation of the co-product lime, however this is associated with additional operational challenges in absorption. These challenges are in higher absorption liquid recirculation rates, due to the moderate pH by the use of gypsum instead to H_2SO_4 and the general difficulty in simultaneously CO_2 and NH_3 absorption. In contrast to the conventional most used air stripping process, vacuum degasification shows promising insights regarding a reduction of the gas-liquid ratio, which is mandatory due to reduced absolute pressure and thereby a reduced pressure loss compared to conventional air stripping.

6. LESSONS LEARNED

The presented ammonia vacuum stripping technology implies several possibly profitable add-ons to the state-of-the-art technologies:

- Reduction in column height: while conventional stripping columns can exceed 10 m in height, calculations show that negative pressure can help to reduce this value depending on elimination target
- The desorption and absorption section profit from different pressure milieus: negative pressure helps remove NH_3 from the digestate, while positive pressure helps fixate it in an absorption fluid. Thus combining conventional absorption with stripping at reduced pressure can achieve a potentially higher process efficiency
- Even though the initial prognosis that the process would not need pretreatment didn't hold true, it still has major advantages regarding the substrate quality over the treatment with membranes or IEX. The small fraction of solids did not impose major problems to the process but they are significant for membrane treatment and IEX.
- It was shown that there is no mandatory need for the use of alkaline substances, when the other process conditions are chosen accordingly. If sufficient thermal energy can be provided on-site, a high process temperature eliminates the need for NaOH.

Since the integrated acidic absorption is a well-researched and field-tested technology, the optimization efforts were put into the more innovative use of gypsum as an alternative source of sulphate for the production of ammonium-sulphate. The cost of gypsum is much lower than that of sulphuric acid and process can capture CO_2 simultaneously:

- Lab tests showed that it's possible to produce ammonium-salts and lime from the ammonia and carbon oxide removed from the digestate
- Integration of a suitable absorption reactor in the pilot system has to happen to test the formation of the desired products
- Large-scale use of gypsum as a sulphate source has been shown before, but it is not a widely applied process

Further research needs to be conducted to fully quantify the technology and applicability of vacuum degasification for nitrogen removal and recovery:

- Given the scale and TRL of the pilot installation it is yet too early to conclusively quantify the degree of improvement over conventional air stripping
- Scale-up needs to happen to compare the system to industrial scale installations of other state-of-the-art solutions
- The reconstructed system needs to be put to test to verify the imputed results
    - The internal energy recovery through steam absorption has to be tested
- The TRL at the end of the project was determined as 5, leaning to 6 according to the TRL assessment tool of the EU [19]

7. LITERATURE

1. Driessen, P., *Nutrient demand and fertilizer requirements*, in *Modelling of agricultural production: weather, soils and crops*. 1986, Pudoc. p. 182-200.
2. Yenigün, O. and B. Demirel, *Ammonia inhibition in anaerobic digestion: A review.* Process Biochemistry, 2013. **48**(5): p. 901-911.
3. Wrage, N., et al., *Role of nitrifier denitrification in the production of nitrous oxide.* Soil Biology and Biochemistry, 2001. **33**(12): p. 1723-1732.
4. Traksel, B.F.G.S.L., *Planning and Design of a full full-scale membrane ammonia stripping*, in *Nitrogen management in side stream*, EAWAG, Editor. 2016: POWERSTEP_EU.
5. Vaneeckhaute, C., et al., *Nutrient Recovery from Digestate: Systematic Technology Review and Product Classification.* Waste and Biomass Valorization, 2016. **8**(1): p. 21-40.
6. Wu, H. and C. Vaneeckhaute, *Nutrient Recovery from Wastewater: A Review on the Integrated Physiochemical Technologies of Ammonia Stripping, Adsorption and Struvite Precipitation.* Chemical Engineering Journal, 2021. **433**: p. 133664.
7. Beckmann, D., *Untersuchungen zum Kalk-Kohlensäure-Gleichgewicht*, in *Angewandte Biowissenschaften und Prozesstechnik*. 2015, Hochschule Anhalt.
8. Ukwuani, A.T. and W. Tao, *Developing a vacuum thermal stripping - acid absorption process for ammonia recovery from anaerobic digester effluent.* Water Res, 2016. **106**: p. 108-115.
9. Koslowski, J., *Inbetriebnahme einer Versuchsanlage zur Rückgewinnung von Ammoniak aus landwirtschaftlichen Gärresten*, in *Umweltverfahrenstechnik*. 2021, Technische Universität Berlin.
10. Sander, R., *Compilation of Henry's law constants (version 4.0) for water as solvent.* Atmospheric Chemistry and Physics, 2015. **15**(8): p. 4399-4981.
11. Nitsche, M., *Kolonnen-Fibel: Für die Praxis im chemischen Anlagenbau*. 2014, Hamburg: Springer Verlag.
12. Dünnebeil, A. *Faulschlamm-Vakuumentgasung*. o. J.; Available from: https://www.pondus-verfahren.de/egas.html.
13. Geist, L., *Optimization of the experimental design of a pilot plant for ammonia vacuum degasification for ammonium sulfate production*, in *Umweltverfahrenstechnik*. 2020, Technische Universität Berlin. p. 91.
14. Koslowski, J., *Inbetriebnahme einer Versuchsanlage zur Rückgewinnung von Ammoniak aus landwirtschaftlichen Gärresten*, in *Institut für Technischen Umweltschutz*. 2021, Technische Universität Berlin. p. 80.
15. Peter, L.-M., *Performance of different condensing setups and operating parameters in ammonia recovery pilot plant with biogas digestate*, in *Umweltverfahrenstechnik*. 2022, Technische Universität Berlin. p. 98.
16. Schwatke, B., *Optimierung einer Vakuumentgasungsanlage zur Stickstoffrückgewinnung aus Gärresten*, in *Verfahrenstechnik*. 2022, Beuth Hochschule für Technik Berlin. p. 79.
17. Rösner, T., *Inbetriebnahme und Optimierungsoptionen eines Ammoniakwäschers bei der Unterdruckentgasung landwirtschaftlicher Gärreste*. 2022, Berliner Hochschule für Technik. p. 103.
18. Meng, M., *Thermisch-alkalisch unterstützte Ammoniakentgasung – Auswirkungen auf das Biomethanpotential von Gärresten*, in *Fachgebiet Umweltverfahrenstechnik*. 2022, Technische Universität Berlin.
19. Union, E., *Horizon Europe TRL Assessment tool.* 2022.
20. Hägg, G., *Die Theoretischen Grundlagen der Analytischen Chemie*. Lehrbücher und Monographien aus dem Gebiete der Exakten Wissenschaften. Vol. 21. 1950, Basel: Springer.
21. Krötz, W., *Systemtechnische Behandlung der Ammoniakemission aus Festmist*, in *Institut für Landtechnik*. 1998, Technische Universität München.
22. Gertz, K.H. and H.H. Loeschcke, *Bestimmung des Diffusionskoeffizienten von CO2 in Wasser.* Zeitschrift für Naturforschung B, 1956. **11**(2): p. 61-64.
23. RVT, *Füllkörper für den Stoff- und Wärmeübergang für höchste Ansprüche der Chemie, Petrochemie und Umwelttechnik*. 2022.

8. ANNEX

7.1. Water and heat balance

The latent heat for water evaporation is described in eq. 10.

$$Q_{vap} = m_{steam} \cdot L_{vap} \qquad \text{eq. 10}$$

Q_{vap}	Required energy for evaporation	kJ	
m_{steam}	Mass of steam (evaporated water)	kg	
L_{vap}	Specific heat for evaporation of water	kJ/kg	2257

This energy is provided through the sensible heat of the system. The sensible heat is described in eq. 11.

$$Q_{heat} = m_{water} \cdot c_p \cdot \Delta T \qquad \text{eq. 11}$$

Q_{heat}	Required energy for heating water	kJ	
m_{water}	Mass of water	kg	
c_p	Specific heat capacity for water	kJ/(kg · K)	4.19
ΔT	Temperature difference	K	

Within our system latent heat and sensible heat are dependend from each other. This means if a certain quantity of steam is generated, the temperature of the remaining water decreases. Meanwhile, when a certain quantity of steam is kondensated, the temperature increases. The correlation between steam flow, water flow and temperature difference can be described in eq. 12 combining eq. 10 and eq. 11.

$$\frac{\dot{m}_{steam}}{\dot{m}_{water}} = \frac{c_p \cdot \Delta T}{L_{vap}} \qquad \text{eq. 12}$$

$\dot{m}_{steam}$	Mass flow of steam	kg/h	
$\dot{m}_{water}$	Mass flow of water	kg/h	
c_p	Specific heat capacity for water	kJ/(kg · K)	4.19
ΔT	Temperature difference	K	
L_{vap}	Specific heat for evaporation of water	kJ/kg	2257

The mass flow of steam is influenced by the mass flow of air and the steam content (see eq. 13). It is assumed that steam is only transported via konvection through the air flow, transport of steam via diffusion and dispersion are neglected.

$$\dot{m}_{steam} = \dot{m}_{air} \cdot \mu \qquad \text{eq. 13}$$

$\dot{m}_{steam}$	Mass flow of steam	$\mathrm{kg/h}$
$\dot{m}_{air}$	Mass flow of air	$\mathrm{kg/h}$
μ	Steam content	$-$

So the relation of gas flow and liquid flow can be expressed via eq. 14

$$\left(\frac{\dot{V}_G}{\dot{V}_L}\right)_{norm} := \frac{\rho_{water,norm}}{\rho_{air,norm}} \cdot \frac{\dot{m}_{air}}{\dot{m}_{water}} = \frac{\rho_{water,norm}}{\rho_{air,norm}} \cdot \frac{c_p \cdot \Delta\mathrm{T}}{L_{vap} \cdot \mu} \qquad \text{eq. 14}$$

$\left(\frac{\dot{V}_G}{\dot{V}_L}\right)_{norm}$	Volumetric Gas-Liquid-ratio under norm-conditions	$-$	
$\rho_{water,norm}$	Density of water under norm-conditions	$\mathrm{kg/m^3}$	1000
$\rho_{air,norm}$	Density of air under norm-conditions	$\mathrm{kg/m^3}$	1.225
$\dot{m}_{air}$	Mass flow of air	$\mathrm{kg/h}$	
$\dot{m}_{steam}$	Mass flow of water	$\mathrm{kg/h}$	
c_p	Specific heat capacity for water	$\mathrm{kJ/(kg \cdot K)}$	4.19
$\Delta\mathrm{T}$	Temperature difference	K	
L_{vap}	Specific heat for evaporation of water	$\mathrm{kJ/kg}$	2257
μ	Steam content	$-$	

The steam content can be calculated via eq. 15 :

$$\mu := \frac{m_{steam}}{m_{air}} = \frac{M_{steam}}{M_{air}} \cdot \frac{e}{p_{abs} - e} = \frac{M_{steam}}{M_{air}} \cdot \frac{1}{\frac{p_{abs}}{e} - 1} \qquad \text{eq. 15}$$

μ	Steam content	$-$
m_{steam}	Mass flow of steam	kg

m_{air}	Mass flow of air	kg	
M_{steam}	Molar mass flow of steam	kg/kmol	18
M_{air}	Molar mass flow of air	kg/kmol	29
e	Vapor pressure of water	mbar	
p_{abs}	Absolute pressure of the system	mbar	

By inserting eq. 15 into eq. 14, eq. 16 results:

$$\left(\frac{\dot{V}_G}{\dot{V}_L}\right)_{norm} = \frac{\rho_{water,norm} \cdot c_p \cdot M_{air}}{\rho_{air,norm} \cdot L_{vap} \cdot M_{steam}} \cdot \Delta T \cdot \left(\frac{p_{abs}}{e} - 1\right) \approx 2{,}442 \frac{1}{K} \cdot \Delta T \cdot \left(\frac{p_{abs}}{e} - 1\right) \quad \text{eq. 16}$$

$\left(\frac{\dot{V}_G}{\dot{V}_L}\right)_{norm}$	Volumetric Gas-Liquid-ratio under norm-conditions	–
ΔT	Temperature difference	K
e	Vapor pressure of water	mbar
p_{abs}	Absolute pressure of the system	mbar

The vapor pressure of water can be calculated via the Magnus equation (eq. 17)

$$e = 6{,}112\ mbar \cdot exp^{\left(\frac{17{,}62 \cdot \vartheta}{243{,}12\ °C + \vartheta}\right)} \quad \text{eq. 17}$$

e	Vapor pressure of water	mbar
ϑ	Temperature	$°C$

By inserting eq. 17 into eq. 16, eq. 18 results:

$$\left(\frac{\dot{V}_G}{\dot{V}_L}\right)_{norm} \approx 2{,}442 \frac{1}{K} \cdot \Delta T \cdot \left(\frac{p_{abs}}{6{,}112\ mbar \cdot exp^{\left(\frac{17{,}62 \cdot \vartheta}{243{,}12\ °C + \vartheta}\right)}} - 1\right) \quad \text{eq. 18}$$

$\left(\frac{\dot{V}_G}{\dot{V}_L}\right)_{norm}$	Volumetric Gas-Liquid-ratio under norm-conditions	–

ΔT	Temperature difference	K
p_{abs}	Absolute pressure of the system	$mbar$
ϑ	Temperature	$°C$

7.2. Buffer capacity

This thereby has practical implications on the buffer capacity for different temperatures. The buffer capacity can be calculated with eq. 19 [20]:

$$\beta = \sum 2.3 \cdot \gamma_A \cdot \gamma_B \cdot c \qquad \text{eq. 19}$$

β	Buffer capacity	$mol/(L \cdot pH)$
γ_A	Molar fraction of acid in relation to total substance	mol/mol
γ_B	Molar fraction of base in relation to total substance	mol/mol
c	Total concentration of substance	mol/L

For the molar fraction of the acid, eq. 20 is given [20]:

$$\gamma_A = \frac{1}{1 + 10^{pH - pK_A}} \qquad \text{eq. 20}$$

γ_A	Molar fraction of acid in relation to total substance	mol/mol
pH	pH-value	$-$
pK_A	pK_A-value	$-$

For the molar fraction of the base, eq. 21 is given [20]:

$$\gamma_B = \frac{1}{1 + 10^{pK_A - pH}} \qquad \text{eq. 21}$$

γ_B	Molar fraction of base in relation to total substance	mol/mol
pH	pH-value	$-$
pK_A	pK_A-value	$-$

7.3. Calculation of height of packings

From the equilibrium and the operation line the recovery degree can be calculated according to eq. 22 and eq. 23 [11].

$$R_d = \frac{x_{in,d} - \frac{y_{in,d}}{m_{eq,d}}}{x_{out,d} - \frac{y_{in,d}}{m_{eq,d}}} \quad \text{eq. 22}$$

R_d	Recovery degree of desorption stage	–
$x_{in,d}$	Influent concentration in the liquid in desorption	mol/mol
$x_{out,d}$	Effluent concentration in the liquid in desorption	mol/mol
$y_{in,d}$	Influent concentration in the gas in desorption	mol/mol
$m_{eq,d}$	Gradient of the equilibrium line for desorption	–

$$R_a = \frac{y_{in,a} - x_{in,a} \cdot m_{eq,a}}{y_{out,a} - x_{in,a} \cdot m_{eq,a}} \quad \text{eq. 23}$$

R_a	Recovery degree of absorption stage	–
$x_{in,a}$	Influent concentration in the liquid in absorption	mol/mol
$y_{in,a}$	Influent concentration in the gas in absorption	mol/mol
$y_{out,a}$	Effluent concentration in the gas in absorption	mol/mol
$m_{eq,a}$	Gradient of the equilibrium line for absorption	–

In terms of desorption with a cleaning gas without the specific substance or in terms of absorption with a cleaning liquid without the specific substance (unloaded gas, unloaded liquid), the recovery degree can be simplified and is directly related to the recovery rate of the desorption or absorption stage (see eq. 24 and eq. 25) [11].

$$R_{d,0} = \frac{x_{in,d}}{x_{out,d}} = \frac{1}{1 - r_d} \quad \text{eq. 24}$$

$R_{d,0}$	Recovery degree of desorption stage for unloaded gas	–
$x_{in,d}$	Influent concentration in the liquid in desorption	mol/mol
$x_{out,d}$	Effluent concentration in the liquid in desorption	mol/mol

r_d	Recovery rate in desorption	–

$$R_{a,0} = \frac{y_{in,a}}{y_{out,a}} = \frac{1}{1 - r_a} \quad \text{eq. 25}$$

$R_{a,0}$	Recovery degree of absorption stage for unloaded liquid	–
$x_{in,a}$	Influent concentration in the gas in absorption	$\mathrm{mol/mol}$
$x_{out,a}$	Effluent concentration in the gas in absorption	$\mathrm{mol/mol}$
r_a	Recovery rate in absorption	–

The stripping factor – a relationship between gradients of equilibrium and operation line – can be calculated according to eq. 26. The stripping factor should be $S_d > 1$ for desorption and $S_a < 1$ for absorption [11].

$$S = m_{eq} \cdot \frac{G}{L} \quad \text{eq. 26}$$

S	Stripping factor for desorption or absorption	–
m_{eq}	Gradient of the equilibrium line for desorption or absorption	–
G	Gas load	$\mathrm{kmol/h}$
L	Liquid load in the desorption or absorption stage	$\mathrm{kmol/h}$

Based on the the recovery degree and stripping factor the number of theoretical plates can be calculated (see eq. 27 and eq. 28) [11].

$$NT_d = \frac{log\left[\left(1 - \frac{1}{S_d}\right) \cdot R_d + \frac{1}{S_d}\right]}{\log(S_d)} \quad \text{eq. 27}$$

$$NT_a = \frac{log[(1 - S_a) \cdot R_a + S_a]}{\log\left(\frac{1}{S_a}\right)} \quad \text{eq. 28}$$

NT	Number of theoretical plates for desorption or absorption	–
S	Stripping factor for desorption or absorption	–

R	Recovery degree of desorption or absorption stage	–

The calculated height of packings is the product from the number of theoretical plates and the height equivalent for one theoretical plate (see eq. 29) [11]

$$H_{fill} = NT \cdot HETP \quad \text{eq. 29}$$

H_{fill}	Height of packings for desorption or absorption	m
NT	Number of theoretical plates for desorption or absorption	–
$HETP$	Height equivalent for one theoretical plate for desorption or absorption	m

The height of one theoretical plate is dependent from the stripping factor the necessary height of packings for the liquid- and gas-side mass transfer (see eq. 30) [11]

$$HETP = \frac{\ln(S)}{S-1} \cdot (S \cdot HTU_L + HTU_G) \quad \text{eq. 30}$$

$HETP$	Height equivalent for one theoretical plate for desorption or absorption	m
S	Stripping factor for desorption or absorption	–
HTU_L	Necessary height of packings for the liquid-side mass transfer for desorption or absorption	m
HTU_G	Necessary height of packings for the gas-side mass transfer for desorption or absorption	m

The necessary height of packings for the liquid-side mass transfer is defined in eq. 31 and for the gas-side mass transfer is defined in eq. 32 [11]

$$HTU_L = \frac{w_L}{\beta_L \cdot a_{Ph}} \quad \text{eq. 31}$$

HTU_L	Necessary height of packings for the liquid-side mass transfer for desorption or absorption	m
w_L	Velocity of liquid in the desorption or absorption column	m/s
β_L	Liquid-side mass transfer coefficient for desorption or absorption	m/s

a_{Ph}	Phase transfer area for desorption or absorption	$\mathrm{m^2/m^3}$

$$HTU_G = \frac{w_G}{\beta_G \cdot a_{Ph}} \quad \text{eq. 32}$$

HTU_G	Necessary height of packings for the gas-side mass transfer for desorption or absorption	m
w_G	Velocity of gas in the desorption or absorption column	$\mathrm{m/s}$
β_G	Gas-side mass transfer coefficient for desorption or absorption	$\mathrm{m/s}$
a_{Ph}	Phase transfer area for desorption or absorption	$\mathrm{m^2/m^3}$

The velocity of gas and liquid is dependend from the gas load/ the liquid load in desorption or absorption stage and the cross-sectional area of the desorption or absoroption column. The liquid is an incompressible fluid, while the gas is a compressible fluid and thereby dependend from the absolute pressure in the column [11].

$$w_L = \frac{\dot{V}_L \cdot \frac{1h}{3600s}}{A} = \frac{L \cdot M_L \cdot 1h}{\rho_L \cdot 3600s \cdot 3.14 \cdot r^2} \quad \text{eq. 33}$$

w_L	Velocity of the liquid in the desorption or absorption column	$\mathrm{m/s}$	
$\dot{V}_L$	Volume flow of the liquid in desorption or absorption column	$\mathrm{m^3/h}$	
A	Cross sectional area in desorption or absorption column	$\mathrm{m^2}$	
L	Liquid load in the desorption or absorption stage	$\mathrm{kmol/h}$	
M_L	Molar mass of liquid (e.g. water)	$\mathrm{kg/kmol}$	18
ρ_L	Density of liquid (e.g. water)	$\mathrm{kg/m^3}$	1000
r	Radius of the desorption or absorption column	m	

$$w_G = \frac{\dot{V}_{G,norm} \cdot \frac{1bar}{p_{abs}} \cdot \frac{1h}{3600s}}{A} = \frac{G \cdot M_G \cdot 1bar \cdot 1h}{\rho_{G,norm} \cdot p_{abs} \cdot 3600s \cdot 3.14 \cdot r^2} \quad \text{eq. 34}$$

w_G	Velocity of the gas in the desorption or absorption column	$\mathrm{m/s}$

$\dot{V}_{G,norm}$	Volume flow of the gas under norm condition of liquid in desorption or absorption column	$\mathrm{m^3/h}$	
p_{abs}	Absolute pressure of the system	bar	
A	Cross sectional area in desorption or absorption column	$\mathrm{m^2}$	
G	Gas load	$\mathrm{kmol/h}$	
M_G	Molar mass of gas (e.g. air)	$\mathrm{kg/kmol}$	29
$\rho_{G,norm}$	Density of gas under norm conditions (e.g. air)	$\mathrm{kg/m^3}$	1.225
r	Radius of the desorption or absorption column	m	

In terms of the phase transfer area the Onda correlation is given in eq. 35[11].

$$a_{Ph} = a \cdot \left[1 - exp\left(-1.45 \cdot \left(\frac{\sigma_{fill}}{\sigma_L}\right)^{0.75} \cdot \left(\frac{w_L}{a \cdot \nu_L}\right)^{0.1} \cdot \left(\frac{{w_L}^2 \cdot a}{g}\right)^{-0.05} \cdot \left(\frac{{w_L}^2 \cdot \rho_L}{\sigma_L \cdot a}\right)^{0.2}\right)\right] \quad \text{eq. 35}$$

a_{Ph}	Phase transfer area for desorption or absorption	$\mathrm{m^2/m^3}$	
a	Specific area of the packings for desorption or absorption	$\mathrm{m^2/m^3}$	
σ_{fill}	Surface tension of the packings for desorption or absorption	$\mathrm{N/m}$	
σ_L	Surface tension of the liquid (e.g. water) in desorption or absorption column	$\mathrm{N/m}$	
w_L	Velocity of the liquid in the desorption or absorption column	$\mathrm{m/s}$	
ν_L	Kinematic viscosity of the liquid (e.g. water) in desorption or absorption column	$\mathrm{m^2/s}$	
g	gravitational acceleration	$\mathrm{m/s^2}$	9.81
ρ_L	Density of liquid (e.g. water)	$\mathrm{kg/m^3}$	1000

The liquid-side mass transfer coefficient is defined in eq. 36 [11]

$$\beta_L = 0.0051 \cdot \left(\frac{D_L}{d_{fill}}\right) \cdot \left(\frac{d_{fill} \cdot g}{{\nu_L}^2}\right)^{1/3} \cdot \left(\frac{w_L}{a \cdot \nu_L}\right)^{2/3} \cdot \left(\frac{a_{Ph}}{a}\right)^{-2/3} \cdot \left(\frac{\nu_L}{D_L}\right)^{0.5} \cdot \left(a \cdot d_{fill}\right)^{0.4} \quad \text{eq. 36}$$

β_L	Liquid-side mass transfer coefficient	$\mathrm{m/s}$
D_L	Liquid diffusion coefficient	$\mathrm{m^2/s}$
d_{fill}	Diameter of packings in desorption or absorption column	m

g	gravitational acceleration	$\mathrm{m/s^2}$	9.81
ν_L	Kinematic viscosity of the liquid (e.g. water) in desorption or absorption column	$\mathrm{m^2/s}$	
w_L	Velocity of the liquid in the desorption or absorption column	$\mathrm{m/s}$	
a	Specific area of the packings for desorption or absorption	$\mathrm{m^2/m^3}$	
a_{Ph}	Phase transfer area for desorption or absorption	$\mathrm{m^2/m^3}$	

The gas-side mass transfer coefficient is definded in eq. 37 [11]

$$\beta_G = 5.23 \cdot \left(\frac{D_G}{d_{fill}}\right) \cdot \left(\frac{\nu_G}{D_G}\right)^{1/3} \cdot \left(\frac{w_G}{a \cdot \nu_G}\right)^{0.7} \cdot \frac{1}{d_{fill} \cdot a} \quad \text{eq. 37}$$

β_G	Gas-side mass transfer coefficient	$\mathrm{m/s}$
D_G	Gas diffusion coefficient	$\mathrm{m^2/s}$
d_{fill}	Diameter of packings in desorption or absorption column	m
ν_G	Kinematic viscosity of the gas (e.g. air) in desorption or absorption column	$\mathrm{m^2/s}$
w_G	Velocity of the gas in the desorption or absorption column	$\mathrm{m/s}$
a	Specific area of the packings for desorption or absorption	$\mathrm{m^2/m^3}$
a_{Ph}	Phase transfer area for desorption or absorption	$\mathrm{m^2/m^3}$

7.4. Calculation of pressure loss among the column

The absolute loss of pressure is defined in eq. 38 [11]

$$\Delta p = \left(\frac{\Delta p}{H}\right)_{wet} \cdot H_{fill} \quad \text{eq. 38}$$

Δp	Absolute pressure loss for desorption or absorption	bar
$\left(\frac{\Delta p}{H}\right)_{wet}$	Height-dependent wet pressure loss for desorption or absorption	$\mathrm{bar/m}$
H_{fill}	Height of packings for desorption or absorption	m

The height-dependent wet pressure loss is defined in eq. 39 [11]

$$\left(\frac{\Delta p}{H}\right)_{wet} = \frac{1\ bar}{10^5\ Pa} \cdot {\Psi_L}^2 \cdot \frac{a}{(\varepsilon - h_L)^3} \cdot \frac{F^2}{2\ m} \cdot \left(\frac{1}{K}\right) \quad \text{eq. 39}$$

$\left(\frac{\Delta p}{H}\right)_{wet}$	Height-dependent wet pressure loss for desorption or absorption	$\mathrm{bar/m}$
Ψ_L	Liquid-side calculation factor for desorption or absorption	–
a	Specific area of the packings for desorption or absorption	–
ε	Porosity of the packings for desorption or absorption	–
h_L	Hold-up of packings for desorption or absorption	–
F	Gas load factor for desorption or absorption	$\sqrt{\mathrm{Pa}}$
$\left(\frac{1}{K}\right)$	Wall factor for desorption or absorption	–

The liquid-side calculation factor for desorption or absorption is calculated via eq. 40 [11]

$$\Psi_L = \Psi_G \cdot exp\left(\frac{Re_L}{200}\right) \cdot \left(\frac{\varepsilon - h_L}{\varepsilon}\right)^{1.5} \cdot \quad \text{eq. 40}$$

Ψ_L	Liquid-side calculation factor for desorption or absorption	–
Ψ_G	Gas-side calculation factor for desorption or absorption	–
Re_L	Reynolds number for the liquid	–
ε	Porosity of the packings for desorption or absorption	–
h_L	Hold-up of packings for desorption or absorption	–

The Reynolds number for the liquid is calculated via eq. 41 [11]

$$Re_L = \frac{w_L}{a \cdot \nu_L} \quad \text{eq. 41}$$

Re_L	Reynolds number for the liquid	–
w_L	Velocity of liquid in the desorption or absorption column	$\mathrm{m/s}$
a	Specific area of the packings for desorption or absorption	$\mathrm{m^2/m^3}$

ν_L	Kinematic viscosity of the liquid (e.g. water) in desorption or absorption column	$\mathrm{m^2/s}$

The hold-up of the packings for desorption or absorption is calculated via eq. 42 [11]

$$h_L = \left(\frac{12 \cdot \nu_L \cdot w_L \cdot a^2}{g}\right)^{1/3} \quad \text{eq. 42}$$

h_L	Hold-up of packings for desorption or absorption	$-$	
w_L	Velocity of liquid in the desorption or absorption column	$\mathrm{m/s}$	
a	Specific area of the packings for desorption or absorption	$\mathrm{m^2/m^3}$	
g	gravitational acceleration	$\mathrm{m/s^2}$	9.81
ν_L	Kinematic viscosity of the liquid (e.g. water) in desorption or absorption column	$\mathrm{m^2/s}$	

The gas-side calculation factor for desorption or absorption is calculated via eq. 43 [11]

$$\Psi_G = C_{fill} \cdot \left(\frac{64}{Re_G} + \frac{1.8}{{Re_G}^{0.08}}\right) \quad \text{eq. 43}$$

Ψ_G	Gas-side calculation factor for desorption or absorption	$-$
C_{fill}	Specific constant for packings	$-$
Re_L	Reynolds number for the liquid	$-$
ε	Porosity of the packings for desorption or absorption	$-$
h_L	Hold-up of packings for desorption or absorption	$-$

The Reynolds number for the gas is calculated via eq. 44

$$Re_G = \frac{w_G}{\nu_G} \cdot \frac{6 \cdot d_{col}}{(a \cdot d_{col} + 4)} \quad \text{eq. 44}$$

Re_G	Reynolds number for the gas	$-$
w_G	Velocity of gas in the desorption or absorption column	$\mathrm{m/s}$

d_{col}	Diameter of the desorption or absorption column	m
ν_L	Kinematic viscosity of the liquid (e.g. water) in desorption or absorption column	$\mathrm{m^2/s}$
a	Specific area of the packings for desorption or absorption	$\mathrm{m^2/m^3}$

The gas load factor is defined in eq. 45 [11]

$$F = w_G \cdot (\rho_G)^{0.5} = w_G \cdot \left(\rho_{G,norm} \cdot \frac{p_{abs}}{1\ bar}\right)^{0.5} \quad \text{eq. 45}$$

F	Gas load factor	$\sqrt{\mathrm{Pa}}$	
w_G	Velocity of gas in the desorption or absorption column	$\mathrm{m/s}$	
ρ_G	Density of gas under pressure conditions in the column	$\mathrm{kg/m^3}$	
$\rho_{G,norm}$	Density of gas under norm conditions (e.g. air)	$\mathrm{kg/m^3}$	1.225
p_{abs}	Absolute pressure of the system	bar	

The wall factor is defined in eq. 46 [11]

$$\left(\frac{1}{K}\right) = 1 + \frac{4}{a \cdot d_{col}} \quad \text{eq. 46}$$

$\left(\frac{1}{K}\right)$	Wall factor for desorption or absorption	$-$
a	Specific area of the packings for desorption or absorption	$\mathrm{m^2/m^3}$
d_{col}	Diameter of the desorption or absorption column	m

7.5. Specific parameter and their dependence from temperature

The liquid-side and gas-side masss transfers as well as the phase transfer area are dependent from the surface tension of the liquid (e.g. water), the kinematic viscosity of the liquid (e.g. water) and the gas (e.g. air) and the liquid and gas diffusion coefficients, which are all dependend from the temperature. The correlations are illustrated in the following sub-chapters.

Surface tention of water

Table 24 shows the temperature dependence of the surface tension of water .

Table 24: Temperature dependency of surface tension of water

Theta [°C]	10	20	30	40	50	60	70	80

σ_L [N/m]	$7.42 \cdot 10^{-2}$	$7.27 \cdot 10^{-2}$	$7.12 \cdot 10^{-2}$	$6.96 \cdot 10^{-2}$	$6.80 \cdot 10^{-2}$	$6.62 \cdot 10^{-2}$	$6.45 \cdot 10^{-2}$	$6.27 \cdot 10^{-2}$

With increasing temperature, the surface tension of water decreases, so the phase transfer increases and the necessary height of packings for the liquid-side and gas-side mass transfer decrease and therefore the absolute height of packings for a fixed recovery degree is reduced.

$$\vartheta \nearrow \Longrightarrow \sigma_L \searrow \Longrightarrow a_{Ph} \nearrow \Longrightarrow HTU_L, HTU_G \searrow \Longrightarrow HETP, H_{fill} \searrow$$

Kinematic viscosity of water

Table 25 shows the temperature dependence of the kinematic viscosity of water and air.

Table 25: Temperature dependency of kinematic viscosity of water and air

Theta [°C]	**10**	**20**	**30**	**40**	**50**	**60**	**70**	**80**
v_L [m²/s]	$1.31 \cdot 10^{-6}$	$1.00 \cdot 10^{-6}$	$8.01 \cdot 10^{-7}$	$6.58 \cdot 10^{-7}$	$5.53 \cdot 10^{-7}$	$4.74 \cdot 10^{-7}$	$4.14 \cdot 10^{-7}$	$3.64 \cdot 10^{-7}$
v_G [m²/s]	$1.43 \cdot 10^{-5}$	$1.52 \cdot 10^{-5}$	$1.61 \cdot 10^{-5}$	$1.70 \cdot 10^{-5}$	$1.80 \cdot 10^{-5}$	$1.90 \cdot 10^{-5}$	$2.00 \cdot 10^{-5}$	$2.10 \cdot 10^{-5}$

With increasing temperature, the kinematic viscosity of water decreases, so the liquid side mass transfer increases and the necessary height of packings for the liquid-side decreases and therefore the absolute height of packings for a fixed recovery degree is reduced.

$$\vartheta \nearrow \Longrightarrow \nu_L \searrow \Longrightarrow \beta_L \nearrow \Longrightarrow HTU_L \searrow \Longrightarrow HETP, H_{fill} \searrow$$

With increasing temperature, the kinematic viscosity of water increase, so the gas side mass transfer decreases and the necessary height of packings for the gas-side increases and therefore the absolute height of packings for a fixed recovery degree is increased.

$$\vartheta \nearrow \Longrightarrow \nu_G \nearrow \Longrightarrow \beta_G \searrow \Longrightarrow HTU_G \nearrow \Longrightarrow HETP, H_{fill} \nearrow$$

Overall, the decrease in the kinematic viscosity of water has superioir effects, so the abosulte height of packings for a fixed recovery degree decreases with increasing temperature.

$$\vartheta \nearrow \Longrightarrow \nu_L \searrow, \nu_G \nearrow \Longrightarrow HETP, H_{fill} \searrow$$

The temperature-impact by viscosity has some impact on the pressure loss, however the pressure loss is more heavily influenced by other parameters, such as the gas or liquid velocity.

$$\vartheta \nearrow \Longrightarrow \nu_L \searrow, \nu_G \nearrow \Longrightarrow Re_G, h_L \searrow, Re_L, \Psi_G, \Psi_L \nearrow \Longrightarrow \left(\frac{\Delta p}{H}\right)_{wet} \nearrow$$

Liquid and Gas diffusion coefficients

Table 26 shows the temperature dependence of the diffusion coefficients of ammonia and carbon dioxide in water and air. [21, 22]

Table 26: Temperature dependency of liquid and gas diffusion coefficients of ammonia and carbon dioxide in water and air [21, 22]

Theta [°C]	**10**	**20**	**30**	**40**	**50**	**60**	**70**	**80**
D_L NH_3 [m²/s]	$1.32 \cdot 10^{-9}$	$1.77 \cdot 10^{-9}$	$2.38 \cdot 10^{-9}$	$3.20 \cdot 10^{-9}$	$4.90 \cdot 10^{-9}$	$5.77 \cdot 10^{-9}$	$7.76 \cdot 10^{-9}$	$1.04 \cdot 10^{-8}$
D_L CO_2 [m²/s]	$1.32 \cdot 10^{-9}$	$1.70 \cdot 10^{-9}$	$2.16 \cdot 10^{-9}$	$2.70 \cdot 10^{-9}$	$3.33 \cdot 10^{-9}$	$4.06 \cdot 10^{-9}$	$4.88 \cdot 10^{-9}$	$5.82 \cdot 10^{-9}$
D_G NH_3 [m²/s]	$1.26 \cdot 10^{-5}$	$1.70 \cdot 10^{-5}$	$2.28 \cdot 10^{-5}$	$3.07 \cdot 10^{-5}$	$4.13 \cdot 10^{-5}$	$5.55 \cdot 10^{-5}$	$7.45 \cdot 10^{-5}$	$1.00 \cdot 10^{-4}$
D_G CO_2 [m²/s]	$1.47 \cdot 10^{-5}$	$1.58 \cdot 10^{-5}$	$1.70 \cdot 10^{-5}$	$1.81 \cdot 10^{-5}$	$1.93 \cdot 10^{-5}$	$2.04 \cdot 10^{-5}$	$2.00 \cdot 10^{-5}$	$2.10 \cdot 10^{-5}$

With increasing temperature, all diffusion coefficients increase, so the gas-side and liquid-side mass transfer increases and the necessary height of packings for the liquid-side decreases and therefore the absolute height of packings for a fixed recovery degree is reduced.

$$\vartheta \nearrow \Longrightarrow D_L, D_G \nearrow \Longrightarrow \beta_L, \beta_G \nearrow \Longrightarrow HTU_L, HTU_G \searrow \Longrightarrow HETP, H_{fill} \searrow$$

7.6. Specific parameter of packings and their impact on operation

Table 27 shows the specific are, the surface tension, the packings constant, the porosity and the diameter of packings for different materials with an diameter between 1.5 and 2 mm suitable for the column in the pilot plant.

Table 27: Different type of packings, their specific area, surface tension of materials, packings constant, porosity and diameter [23]

Type of packing	a	σ_{fill}	C_{fill}	ε_{fill}	d_{fill}
-	m^2/m^3	N/m	-	-	m
Steel 15-3 Raflux	360	$7.10 \cdot 10^{-2}$	0,57	0,96	$15 \cdot 10^{-3}$
PP 15-7 Highflow	313	$4.00 \cdot 10^{-2}$	0,57	0,91	$15 \cdot 10^{-3}$
Steel 50-5 Raflux	112	$7.10 \cdot 10^{-2}$	0,57	0,97	$50 \cdot 10^{-3}$
PP 50-3 Highflow	95	$4.00 \cdot 10^{-2}$	0,57	0,94	$50 \cdot 10^{-3}$
Steel 90-8 Raflux	65	$7.10 \cdot 10^{-2}$	0,57	0,98	$90 \cdot 10^{-3}$
PP 90-7 Highflow	76	$4.00 \cdot 10^{-2}$	0,57	0,97	$90 \cdot 10^{-3}$

With increasing specific area of the packings the phase transfer area increases, however the liquid- and gas-side mass transfer coefficient decrease, which have an superior effect on the necessary high of packings, so the overall high of packings increases.

$$a \nearrow \Longrightarrow a_{Ph} \nearrow, \beta_L, \beta_G \searrow \Longrightarrow NTU_L, NTU_G \nearrow \Longrightarrow HETP, H_{fill} \nearrow$$

In terms of the specific area of the packings and the pressure loss, their are variable relations depending on the exact operational parameters. No definite relations can be described.

With increasing surface tension of the packings, the phase transfer area of the packings increase, so the necessary of high of packings and the overall high of packings decreases.

$$\sigma_{fill} \nearrow \Longrightarrow a_{Ph} \nearrow \Longrightarrow HTU_L, HTU_G \searrow \Longrightarrow HETP, H_{fill} \searrow$$

With increasing diameter of packings the liquid- and gas-side mass transfer coefficent decreases, so the necessary high of packings and the overall high of packings increases.

$$d_{fill} \nearrow \Longrightarrow \beta_L, \beta_G \searrow \Longrightarrow NTU_L, NTU_G \nearrow \Longrightarrow HETP, H_{fill} \nearrow$$

With increasing porosity of packings, the pressure loss decreases.

$$\varepsilon_{fill} \nearrow \Longrightarrow \Psi_L \nearrow \Longrightarrow \left(\frac{\Delta p}{H}\right)_{wet} \searrow$$